

A conserved metabolic signature associated with response to fast-acting anti-malarial agents

Nelson V. Simwela,¹ W. Armand Guiguemde,² Judith Straimer,² Clement Regnault,¹ Barbara H. Stokes,¹ Luis E. Tavernelli,¹ Fumiaki Yokokawa,² Benjamin Taft,² Thierry T. Diagana,² Michael P. Barrett,¹ Andrew P. Waters¹

AUTHOR AFFILIATIONS See affiliation list on p. 19.

ABSTRACT Characterizing the mode of action of anti-malarial compounds that emerge from high-throughput phenotypic screens is central to understanding how parasite resistance to these drugs can emerge. Here, we have employed untargeted metabolomics to inform on the mechanism of action of anti-malarial leads with different speed of kill profiles being developed by the Novartis Institute of Tropical Diseases (NITD). Time-resolved global changes in malaria parasite metabolite profiles upon drug treatment were quantified using liquid chromatography-based mass spectrometry and compared to untreated controls. Using this approach, we confirmed previously reported metabolomics profiles of the fast-killing (2.5 h) drug dihydroartemisinin (DHA) and the slower killing atovaquone. A slow-acting anti-malarial lead from NITD of imidazolopiperazine (IZP) class, GNF179, elicited little or no discernable metabolic change in malaria parasites in the same 2.5-h window of drug exposure. In contrast, fast-killing drugs, DHA and the spiroindolone (NITD246), elicited similar metabolomic profiles both in terms of kinetics and content. DHA and NITD246 induced peptide losses consistent with disruption of hemoglobin catabolism and also interfered with the pyrimidine biosynthesis pathway. Two members of the recently described class of anti-malarial agents of the 5-aryl-2-amino-imidazothiadiazole class also exhibited a fast-acting profile that featured peptide losses indicative of disrupted hemoglobin catabolism. Our screen demonstrates that structurally unrelated, fast-acting anti-malarial compounds generate similar biochemical signatures in *Plasmodium* pointing to a common mechanism associated with rapid parasite death. These profiles may be used to identify and possibly predict the mode of action of other fast-acting drug candidates.

IMPORTANCE In malaria drug discovery, understanding the mode of action of lead compounds is important as it helps in predicting the potential emergence of drug resistance in the field when these drugs are eventually deployed. In this study, we have employed metabolomics technologies to characterize the potential targets of anti-malarial drug candidates in the developmental pipeline at NITD. We show that NITD fast-acting leads belonging to spiroindolone and imidazothiadiazole class induce a common biochemical theme in drug-exposed malaria parasites which is similar to another fast-acting, clinically available drug, DHA. These biochemical features which are absent in a slower acting NITD lead (GNF17) point to hemoglobin digestion and inhibition of the pyrimidine pathway as potential action points for these drugs. These biochemical themes can be used to identify and inform on the mode of action of fast drug candidates of similar profiles in future drug discovery programs.

KEYWORDS anti-malarial agents, malaria, metabolomics, *Plasmodium falciparum*

Malaria is a resurgent worldwide public health problem affecting millions and, in the case of *Plasmodium falciparum*, killing hundreds of thousands of people annually

Editor Vasant Muralidharan, University of Georgia, Athens, Georgia, USA

Address correspondence to Andrew P. Waters, andy.waters@glasgow.ac.uk.

The authors declare no conflict of interest.

See the funding table on p. 19.

Received 2 October 2022

Accepted 27 January 2023

Published 6 October 2023

Copyright © 2023 Simwela et al. This is an open-access article distributed under the terms of the [Creative Commons Attribution 4.0 International license](https://creativecommons.org/licenses/by/4.0/).

(1). Central to malaria control programs are anti-malarial drugs, which form crucial components of the current malaria treatment, prophylaxis, and transmission blocking strategies. Artemisinins (ARTs), in artemisinin combinational therapies (ACTs), have been the backbone of these strategies in the last decade and have contributed significantly to the recent gains achieved in malaria control (1, 2). ACTs currently remain mostly effective in sub-Saharan Africa, a region that harbors the highest burden of the disease. However, as has been the historical trend with anti-malarial treatments, resistance to ARTs emerged in Southeast Asia (SEA) and was first reported in 2009 along the Thai-Cambodian border (3). At present, ART treatment failure has reached endemic status in SEA (1, 4, 5) and has seemingly emerged in Africa (6). More worryingly, parasites carrying both ART and partner drug piperazine resistance mutations have been reported in SEA, threatening the current mainstay of ACTs (7, 8). Pipelines to identify new drugs to combat the emerging resistance or for effective combination therapies are thus urgently needed.

Over the past decade, thousands of chemical entities that block malaria parasite growth have been reported from pharmaceutical companies and public-funded product development partnerships (9–11). These screens have provided appropriate starting points for anti-malarial drug discovery which could serve as potential replacements and/or suitable combination partners with current drugs to combat and overcome resistance. However, as is the case with a majority of anti-parasite compounds identified through phenotypic screens against parasites, their mode of action is unknown (12, 13). Characterizing the mode of action of lead drug candidates or drugs that are already in clinical use, though not essential during drug development, is important as it provides a platform to understand or predict resistance mechanisms as well as identify suitable combination drug partners using mode of action informed strategies. Mode of action elucidation also helps in identifying the actual drug targets which can be exploited in structure-based design toward better drugs.

Mode of action elucidation in malaria parasites has primarily involved forward genetics approaches, which involve *in vitro* selection for resistance followed by whole-genome sequencing and transcriptome or proteome analysis. These approaches have identified or confirmed the mechanism of resistance and mode of action of known anti-malarial drugs such as atovaquone (ATQ), pyrimethamine, and chloroquine (14–16). They have also pointed to potential molecular targets of novel compounds, for example, phosphatidylinositol 4-kinase (17), protein synthesis (18), and the pyrimidine biosynthesis pathways (19). These forward genetic screens, however, have their own limitations as they might not reveal the full range of molecular and biochemical networks involved in drug resistance processes (13). Moreover, these screens cannot be used to probe mode of action of chemical entities when drug resistance cannot be selected (high barrier compounds), drug resistance is phenotypic (20), or when resistance is conferred by gene mutations in multi-drug resistance transporters which provide little or no clue as to the intracellular target of the compounds. Metabolomic screening platforms now provide an alternative approach to elucidating the mode of action of both known drugs and lead candidates in bacterial pathogens (21, 22) and malaria parasites (23–25) as many anti-microbial agents target metabolic enzymes and pathways. This has been made possible because metabolomics platforms can detect perturbations induced by drug treatment under controlled *in vitro* exposure conditions (13, 21, 26). In malaria parasites, these approaches have been used to identify the mode of action of polyamine inhibitors (27), to validate the activity of new quinolone drugs targeting the parasite electron transport chain (28), and to reveal metabolic-specific phenotypes associated with the clinically relevant drugs dihydroartemisinin (DHA) and chloroquine (24, 29). Metabolomic screens of the malaria box compounds have also revealed established as well as novel targets of potential malarial drug candidates (23, 25). Combinatorial -omics approaches can provide even greater detail, as, for example, high-resolution metabolomics combined with peptidomics, and biochemical analyses revealed that a novel fast-acting lead drug candidate being developed by the Medicines for Malaria

Venture (JPC-3210, MMV 892646) possibly acts by inhibiting hemoglobin catabolism and protein translation (30). Metabolomic approaches are also, successfully, being integrated in early stages of drug discovery programs to predict the mode of action of novel anti-malarial agents as has been reported by the target guided Malaria Drug Accelerator consortium (31, 32).

In this study, an untargeted metabolomics approach was used to screen two novel fast-acting drug candidates of the 5-aryl-2-amino-imidazothiazole (ITD) class that have emerged from the Novartis Institute of Tropical Diseases (NITD) drug discovery pipelines (33). We first validated our metabolic profiles using ATQ, which has a well-characterized metabolic fingerprint (23, 24). Thereafter, the metabolic profile of two representatives of the ITD compound series, Cpd 9 and Cpd 55 (33), was compared to other drug candidates from the NITD pipeline: spiroindolones (NITD246), which are known to target the *P. falciparum* Na⁺ H⁺ ATPase (PfATP4) (34) and GNF179 (KAF156 analog), whose precise mode of action is still unknown (35–37). These profiles were further compared to that of the lead fast-acting anti-malarial DHA using a fixed time point as well as a dynamic time course over the first 2.5 h of drug exposure. We demonstrate that the metabolic profile of the fast-acting anti-malarial drugs and drug candidates tested here, of greatly differing chemical structure, reveals fundamental similarities in their impact on the parasite, interfering with hemoglobin catabolism. We conclude that this could be a common metabolic response of the parasites which reflects either a commonality in the mode of action or a common parasite response to rapidly induced death.

RESULTS AND DISCUSSION

ITDs display a fast-killing rate

Parasite killing rates allow for identification of fast-acting compounds which are desirable for malaria control as they allow for rapid clearance of parasitemia in patients, which in turn minimizes parasite drug exposure time and narrows the window in which parasites can evolve resistance. *In vitro* assays to predict the parasite killing rates of anti-malarial compounds are based on parasite reduction ratios (PRRs), quantified over 28 days by fresh exposure of a defined parasite inoculum every 24 h in a series of limiting dilutions (38). Even though the PRR method allows for determination of parasite clearance times as well as drug lag phases (the time required for compounds to achieve maximum killing effect), the extent to which parasite metabolic and biochemical fingerprints change, especially for potentially pleiotropic, fast-acting compounds where the onset of action is less than 24 h, cannot be predicted accurately. We determined the killing kinetics of two ITD series of compounds (Cpd 9 and Cpd 55), NITD246, DHA, GNF179, and ATQ by biochemically monitoring luciferase expression using a *P. falciparum* 3D7 luc line which constitutively expresses a dual NanoLuc and luciferase reporter. Synchronized trophozoites at 2% parasitemia and 2% hematocrit were cultured with the compounds at 10 × 72-h half maximal inhibitory concentration (IC₅₀) (Table 1) or dimethyl sulfoxide (DMSO) (0.1%), after which bioluminescence was monitored over the course of 6 h. DHA (1 μM), which is a known fast-acting compound, depleted the luciferase signal after 2.5 h of incubation (Fig. 1A). A member of the spiroindolone series (NITD246) also depleted the signal after 2.5 h but at a faster initial rate than DHA (Fig. 1A). This is in agreement with observations that spiroindolones exert a faster mode of action and parasite clearance than ARTs in patients (39). Meanwhile, both ITDs, Cpd 9 and Cpd 55, at 10 × IC₅₀ displayed an even faster killing rate (with similar kinetics), depleting the luciferase signal after 2 h of drug incubation, in line with previous observations in the PRR assays (33). By contrast, GNF179 and ATQ, which are known to act slowly, had a negligible effect on the luciferase signal over 6 h at 10 × IC₅₀, displaying an almost identical response to the DMSO control. Microscopic analysis of parasite morphologies during the time points did not show any significant differences relative to the DMSO control (Fig. 1B). Based on these data, we chose 2.5 h as our initial first time point for metabolomic drug incubation as it was the time which corresponded with maximal biochemical signal disruption

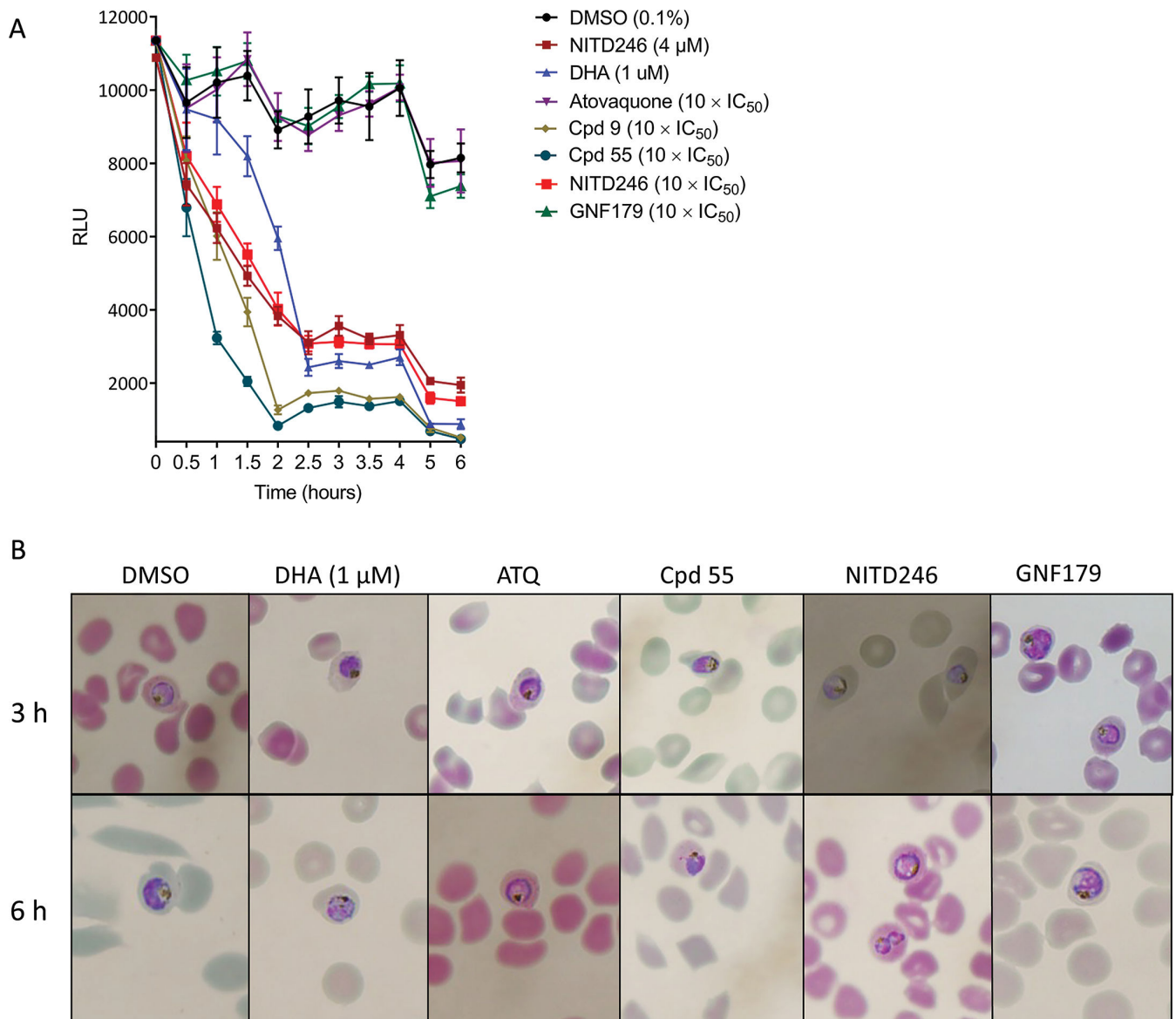


FIG 1 Killing kinetics of NITD246, DHA, ATQ, Cpd 9, Cpd 55, and GNF179 in the 3D7 luc line. Trophozoites ~30 h old at 2% hematocrit and 2% parasitemia were incubated with the compounds at the indicated concentrations or $10 \times IC_{50}$ (Table 1) for the indicated times. Luciferase expression was quantified at each time point. (A) Plot of relative light units (RLU) over the 6-h incubation periods for the compounds. Incubations were carried out in quadruplicate over two independent biological repeats. (B) Microscopy analysis of Giemsa-stained smears at the 3- and 6-h incubation periods for a selected compounds from panel A at the indicated concentrations or $10 \times IC_{50}$.

(based on luciferase expression) for the fast-acting compounds and has been previously shown to yield a good metabolic signal even for slow-acting compounds such as ATQ (23).

ATQ disrupts pyrimidine biosynthesis pathway in malaria parasites

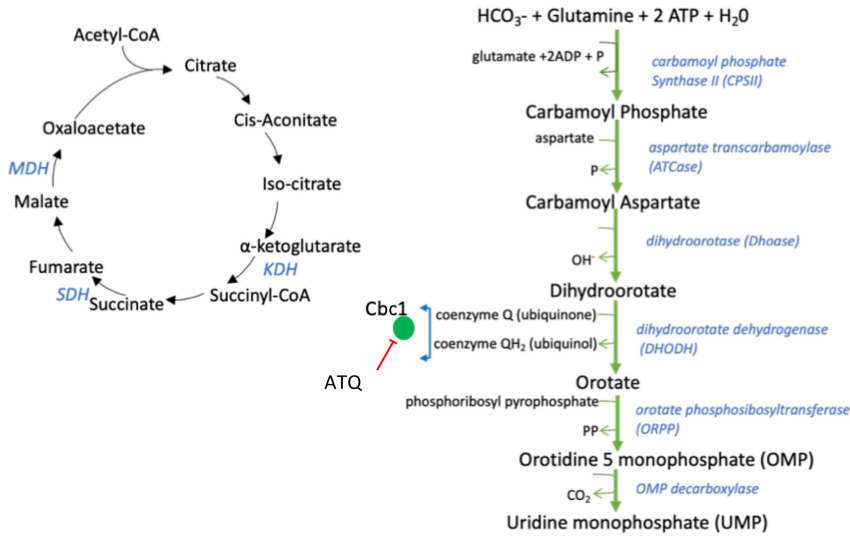
ATQ targets the mitochondrial electron transport chain (mETC) bc1 complex (Cbc1) that plays a crucial role in oxidative phosphorylation in most organisms (40). However, malaria parasites do not require oxidative phosphorylation and have maintained an active mETC in the asexual blood stages for the sole purpose of recycling ubiquinone, which acts as an electron acceptor for dihydroorotate dehydrogenase (DHODH), a critical enzyme in the pyrimidine biosynthesis pathway. The parasite's mETC also indirectly feeds

into the tricarboxylic acid pathway (TCA) by supplying ubiquinone, which is essential for the activity of dehydrogenases of the TCA, succinate dehydrogenase (SDH) and malate dehydrogenase (MDH) (41). Purified trophozoites exposed to ATQ at $10 \times IC_{50}$ for 2.5 h, revealed a rapid accumulation of N-carbamoyl L-aspartate and dihydroorotate while the level of downstream pyrimidine metabolites; uridine diphosphate (UDP) and uridine triphosphate (UTP) declined (Fig. 2A and B; Fig. S1B and C). This is in agreement with previously reported metabolomic profiles for ATQ (23, 24). We also observed that orotate levels were maintained despite DHODH inhibition with ATQ (Fig. S1A) as has also been previously observed (24). The mechanism underlying this phenomenon remains unclear. ATQ treatment also led to a decrease in cellular levels of citrate (Fig. 2B). Blood stage malaria parasites appear to carry out a canonical oxidative TCA where the majority of the carbon enters the cycle as α -ketoglutarate derived from a series of glutaminolytic reactions (42). However, a low flux of glucose-derived carbon into the TCA through acetyl-CoA has also been reported (42, 43). Meanwhile, it has been demonstrated that ATQ resistance (a bypass of mETC inhibition) can be achieved in transgenic malaria parasites that artificially express yeast DHODH, which does not require ubiquinone for its activity (41). Conversely, mETC inhibition by ATQ acts as a *de facto* knockout of all enzymes that require ubiquinone for activity, which include DHODH, SDH, and MDH. Indeed, using the same parasites expressing yeast DHODH which can tolerate otherwise lethal doses of ATQ, stable isotope labeling was used to demonstrate that ATQ activity does not just inhibit the mETC but also prevent flux of glucose-derived carbons into the TCA (44). Previous ATQ metabolomics profiles have also revealed disruption in the TCA cycle as an accumulation of fumarate was observed, consistent with interference of SDH or MDH, as a consequence of Cbc1 complex inhibition (24). Even though we do not observe an accumulation of fumarate in our metabolomic screen (Fig. S1D), which could be due to shorter drug exposure time, a steady decrease in the TCA cycle metabolites, which was previously comprehensively profiled upon stable isotope labeling (24), is mirrored by the observed decrease in levels of citrate in our profiling. Taken together, these results validated our metabolomics approach for mode of action elucidation of selected NITD drug candidates (Table 1).

NITD246 elicits a pleiotropic metabolic response in malaria parasites

NITD246, a spiroindolone analog of KAE609, is one of the fast-acting compounds developed by NITD and has shown promising results in clinical trials (39, 45). Using forward genetic screens after *in vitro* selection for resistance, spiroindolone KAE609 was proposed to target PfATP4, a $Na^+ H^+$ ATPase, even though the exact events preceding parasite death remain unknown (34). Treating malaria parasites with KAE609 has been shown to lead to a rapid influx of sodium, increased rigidity of infected red blood cell (RBC) membranes, and consequent alteration of parasite morphology/rheology (46, 47). We compared the metabolomic profile of *P. falciparum* exposed to NITD246 or its inactive analog, NITD246i, after 2.5 h of incubation with $10 \times IC_{50}$ of NITD246. A massive reduction in peptide levels (many of them potentially hemoglobin derived) was observed (Fig. 3A; Table S1). Moreover, NITD246 incubation resulted in accumulation of choline and glycerophosphocholine (Fig. 3B), disrupted the pyrimidine biosynthesis pathway (but with a different signature to ATQ; Fig. 3C and D; Fig. S2A), and also caused a loss in purine metabolites (Fig. S2B). These data are in contrast to the inactive analogs which yielded profiles similar to the DMSO control. These observations are also similar to previous metabolomic profiles for KAE609 (NITD246) which reported a loss of hemoglobin-derived peptides, amino acid derivatives, and central carbon metabolites (23). This illustrates a potential pleiotropic metabolic response that could arise as a result of rapid disruption of cellular homeostasis upon PfATP4 inhibition and sodium influx. In spite of the evidence indicating that KAE609 targets PfATP4, it remains questionable whether PfATP4 is the direct target of this compound or acts as a multidrug resistance gene. Mutations in *PfATP4* do confer resistance not just to KAE609 but also to a diverse array of chemically unrelated compounds (such as carboximides, aminopyrazoles,

A



B

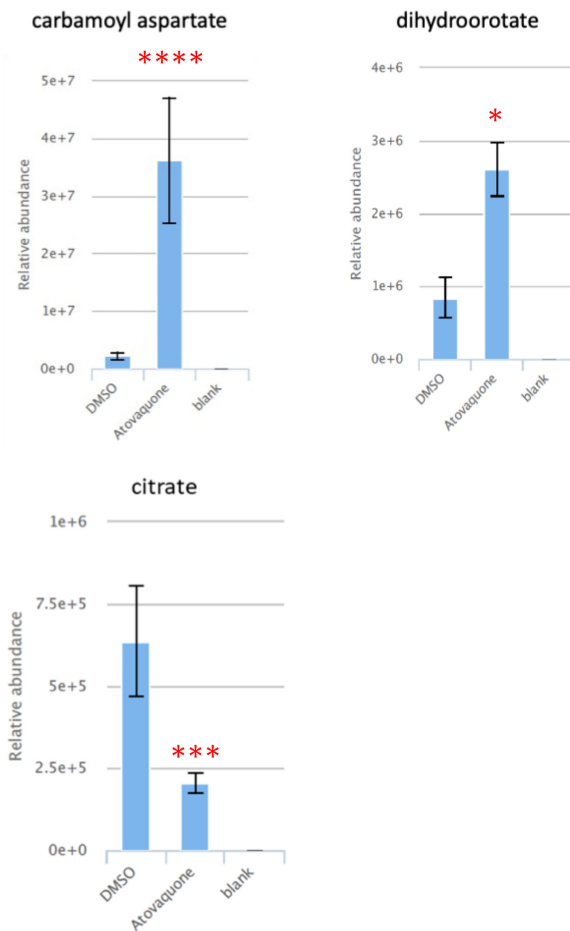


FIG 2 Metabolomic profile of ATQ. Purified trophozoites (~1 × 10⁸) were exposed to either DMSO or ATQ at 10 × IC₅₀ for 2.5 h. Untargeted metabolomics on an LC-MS platform was carried out on extracted metabolites. (A) Schematic of the TCA cycle and pyrimidine pathways. The Cbc1, which is the target (Continued on next page)

FIG 2 (Continued)

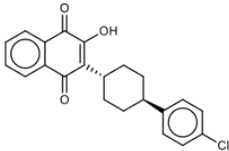
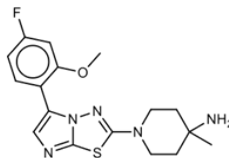
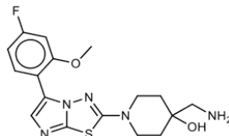
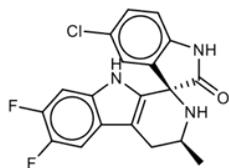
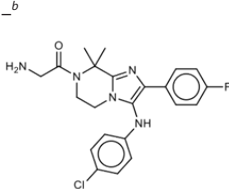
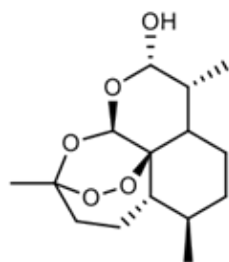
of ATQ, is shown in relation to its role in recycling of ubiquinol for DHODH activity and regeneration in the TCA by indicated dehydrogenases. (B) Relative abundance of the indicated pyrimidine and TCA metabolites in DMSO vs ATQ treatments. Relative abundance measurements are comparisons of total ion counts of the metabolites in the treatment conditions. Treatments were carried out in triplicates over two independent biological repeats. mzXML mass spectrometry files and graphs were processed and plotted in PiMP. Error bars are standard deviations. Significant changes are adjusted *P* values of treatments as compared to DMSO. **P* < 0.05, ****P* < 0.001, *****P* < 0.0001. KDH, ketoglutarate dehydrogenase; MDH, malate dehydrogenase (also called malate quinone oxidoreductase); SDH, succinate dehydrogenase.

pyrazoleamides, and dihydrosioquinolines) which all possess potent anti-malarial activity (48–50). Our metabolomics data point to primary or secondary pleiotropic events associated with exposure to KAE609, including diminished hemoglobin catabolism and the inhibition of pyrimidine biosynthetic pathways which could be part of the mode of action or consequence of NITD246-mediated parasite killing. Interestingly, although the pyrimidine metabolic profile of NITD246 differs from that of ATQ (Fig. 3D), it is similar to the previously reported pyrimidine metabolomic profile of DHA-treated parasites, albeit at differing time points (24). These data suggest that both DHA and spiroindolones directly or indirectly perturb the early enzymes of pyrimidine biosynthesis (ATCase and CPSII), leading to diminished levels of downstream metabolites. In a separate metabolomic profiling of malaria box compounds (25), metabolic fingerprints of DHA-treated parasites were shown to cluster together with KAE609 and also some other PfATP4 inhibitors: SJ733 and MMV006427. The actual events leading to parasite death in NITD246 could thus potentially involve promiscuous unspecific targeting, similar to DHA, shutting down multiple biological pathways in the parasite.

ITD series compound metabolic responses are restricted to peptides

Cpd 9 and Cpd 55 are analogs of the 5-aryl-2-amino-imidazothiadiazole class of compounds that are in the developmental pipeline at the NITD (33). Cpd 55 is a downstream derivative of Cpd 9, both of which are structurally conserved (Table 1) and share comparable parasite kill profiles (Fig. 1A). They are very fast acting (Cpd 9t_{1/2} ~1 h, Cpd 55t_{1/2} <45 min), even more rapid than spiroindolones (NITD246) and DHA (Fig. 1A) (33). Attempts to generate parasite lines highly resistant to these compounds by *in vitro* selection have so far been unsuccessful, making attempts to characterize their mode of action particularly difficult. In our metabolomic screen, Cpd 9 and Cpd 55 induced very similar metabolic profiles, which were almost entirely restricted to significant reductions across predicted peptides (Fig. 4A and B; Tables S2 and S3). Some of these peptides (highlighted in Fig. 4A and B) could be mapped to the α and β chain sequences of hemoglobin, a similar perturbation to that reported previously in metabolic profiling of DHA (24, 25). This would suggest that ITDs potentially target hemoglobin breakdown as they exert their anti-parasite activity. The ITD peptide response appears to be similar to those observed with NITD246 as well as DHA in previous screens (23–25). While DHA has been proposed to target hemoglobin catabolism, NITD246 is believed to target PfATP4 (34); hence, the hemoglobin breakdown response associated with exposure to this drug may be secondary. The ITD peptide response could also be a secondary consequence of related inhibition of a target not revealed by our metabolomic screen. Moreover, the true source of short dipeptides/tripeptides revealed here is difficult to ascertain with certainty. For example, the Met-Ala, Trp-Pro, and Leu-Met peptide combinations, which are also significantly perturbed in the ITDs' metabolic profile (Fig. 4A and B), are not present in hemoglobin sequences. This could point toward a more general inhibition of protein degradation systems, impaired flux of oligopeptides due to inhibition of transporters (51), or a signal of dying parasites that bears no relevance to the target or primary mode of drug action. Several compounds with unrelated primary modes of action (DHA, spiroindolones and aminopyridines; PI4K inhibitors and triaminopyrimidines; vacuolar ATPase inhibitors and chloroquine) have been shown to perturb

TABLE 1 List of anti-malarial compounds used in this study, their structures, and IC₅₀ values^a

Abbreviation	Name	General structure	IC ₅₀ (nM)
ATQ	Atovaquone		1.05 ± 0.03
Cpd 9	ITD series compound 9		31.25 ± 0.83
Cpd 55	ITD series compound 55		24.15 ± 2.06
NITD246	KAE609 analog		0.72 ± 0.04
NITD246i	NITD246 inactive analog	- ^b	143.55 ± 7.75
GNF179	KAF156 analog		27.14 ± 0.61
Cpd 9_ia	Inactive analog of Cpd 9	-	>1,000
Cpd 55_ia	Inactive analog of Cpd 55	-	>1,000
DHA	Dihydroartemisinin		6.23 ± 0.34

^aIC₅₀ values are means and standard deviations from three biological repeats.

^b-, Not applicable

hemoglobin catabolism (23, 52). However, the ITD peptide response we note here is not accompanied by disruption to other pathways such as pyrimidine or purine nucleotide responses, as is the case with NITD246 or DHA. Interestingly, another fast-acting compound that has been developed by the MMV, JPC-3210 (MMV 892646), elicits a similar metabolic response to the ITDs, for example, being mostly restricted to peptides leading to the proposal that inhibited hemoglobin catabolism is its primary mode of action, although interference with protein translation was also noted, which might as well be a feature of ITD activity (30).

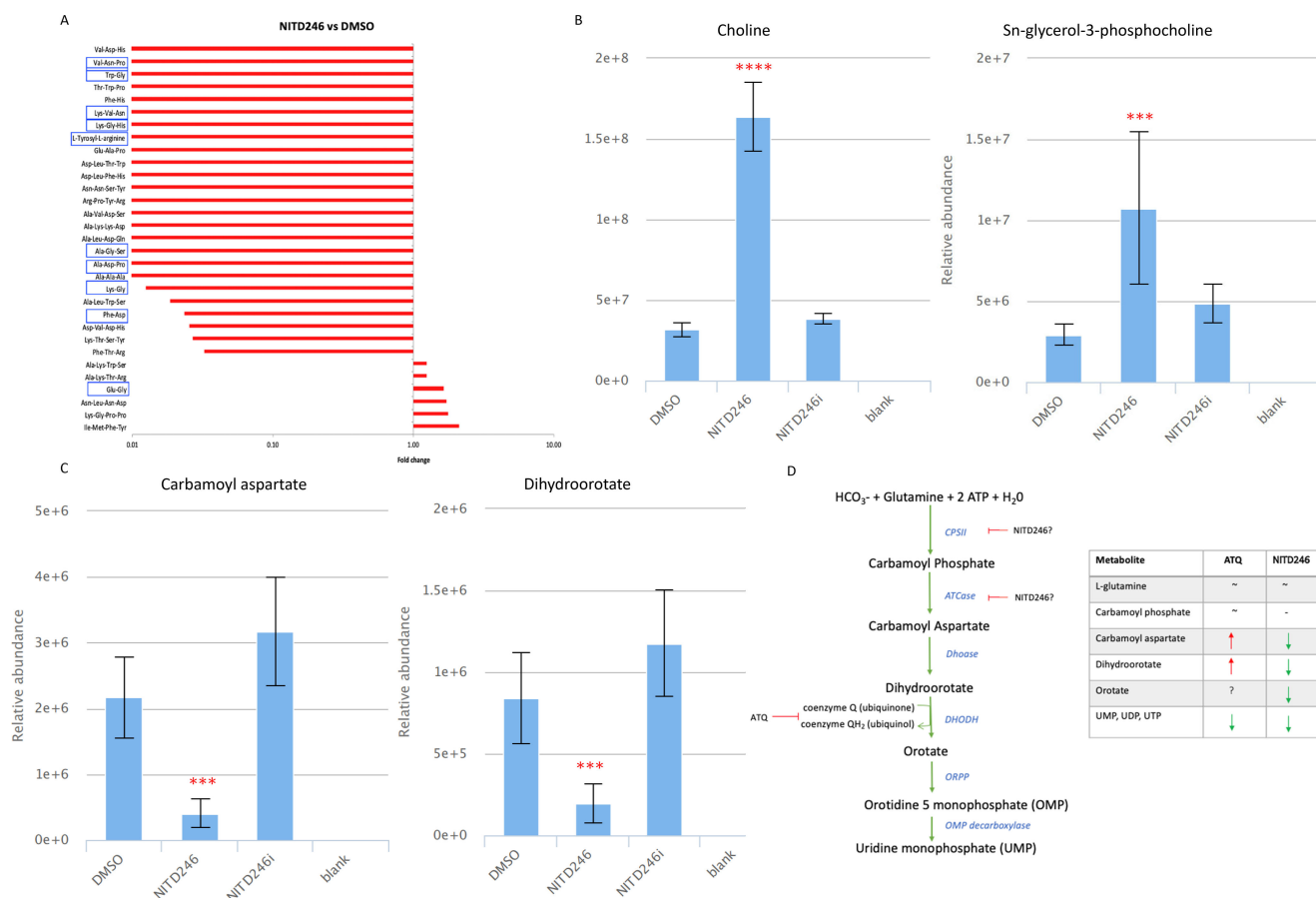


FIG 3 Pleiotropic metabolic response of malaria parasites after exposure to NITD246 for 2.5 h. (A) Global untargeted metabolomic response of selected peptides in NITD246-treated trophozoites as compared to DMSO. Peptides with hemoglobin matching sequences as well as those that are potentially hemoglobin derived (23–25) are highlighted with blue rectangular shapes. (B) Relative abundance of choline and choline derivatives in the NITD246-treated parasites as compared to DMSO and inactive analog. (C) Relative abundance of the indicated pyrimidine biosynthesis pathway metabolites in the NITD246-treated parasites as compared to DMSO and inactive analog. (D) Cartoon of the pyrimidine biosynthesis pathway showing ATQ (Fig. 2) and NITD246 potential action points. The table is a direct comparison of ATQ and NITD246 pyrimidine biosynthesis pathway metabolites. Fold changes (relative to DMSO control) and relative abundance comparisons are means from two biological repeats collected in triplicate at each time of drug incubation. Error bars are standard deviations. Significant changes are adjusted *P* values of treatments as compared to DMSO. ****P* < 0.001, *****P* < 0.0001.

GNF179 elicits minimal discernible impact on the metabolome

KAF156 belongs to the imidazolopiperazine class of compounds that have been developed by the NITD and have shown potential as anti-malarial agents for use in malaria treatment, prophylaxis, and transmission blocking (36, 53). The exact mode of action of KAF156 is currently unknown, but mutations in the *P. falciparum* cyclic amine resistance locus (*PfCARL*) as well as UDP-galactose and acetyl-CoA transporters have all been shown individually to confer resistance to KAF156 and its close analogs (35, 54). In our screen, the KAF156 analog, GNF179, did not induce any significant metabolic effect after incubating parasites with the compound for 2.5 h, consistent with its slower rate of kill. Some low-level, albeit significant, increase in purine metabolites (Fig. 5A) was observed, along with a low-level accumulation of central carbon metabolism metabolites (malate, succinate, and oxoglutarate) (Fig. 5B). This is also in agreement with previously reported metabolomics profiles of KAF156 as no significant changes in the parasite metabolome were observed after the same period of drug incubation (23). It is, therefore, not possible to predict the mode of action of GNF179 based on these profiles. Nevertheless, GNF179 is a relatively slow-acting drug (Fig. 1A), which would suggest that extending exposure beyond 2.5 h may be required to elicit an observable biochemical response,

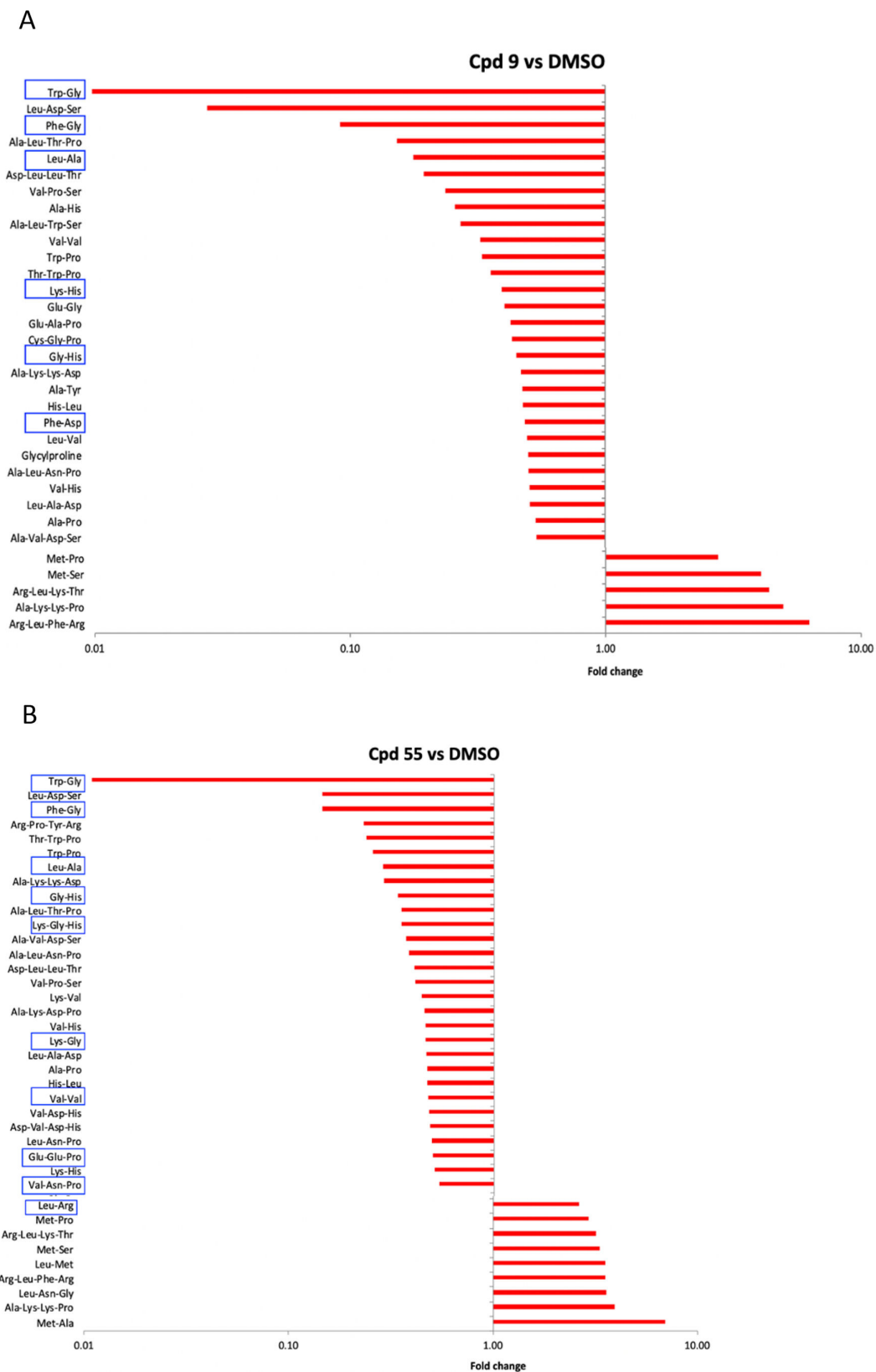


FIG 4 Peptide metabolic responses of the ITD series compounds in malaria parasites. Global response of selected peptides upon treatment with Cpd 9 (A) or Cpd 55 (B). Peptides with hemoglobin matching sequences as well as those which most likely derive from the same (24, 25) are highlighted with blue rectangle shapes. Fold changes relative to the DMSO control are means from two biological repeats collected in triplicate at each time of drug incubation.

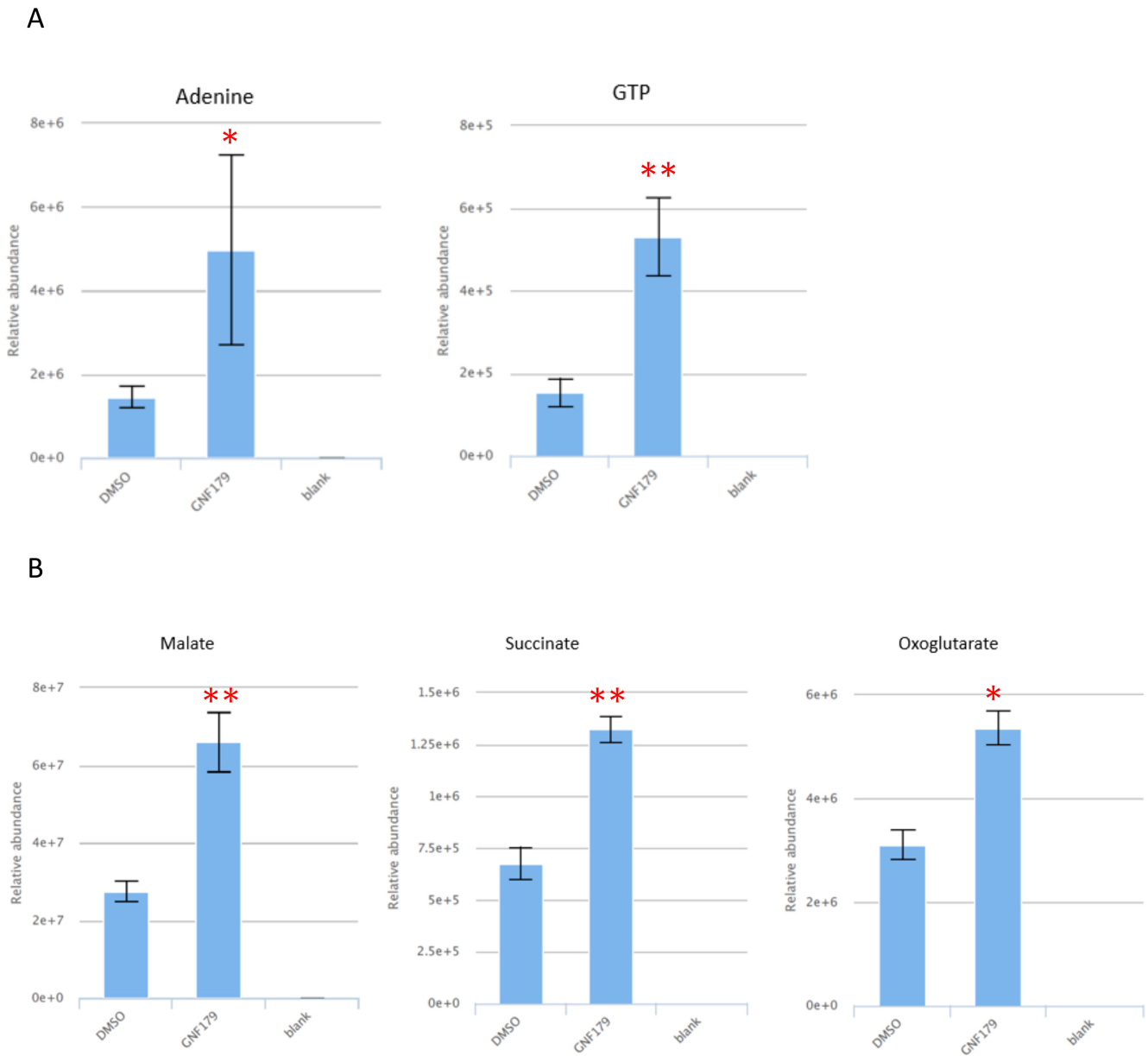


FIG 5 GNF179 metabolomic response for selected metabolites. Relative abundance of adenine, GTP (A), and central carbon metabolism intermediates (B) in GNF179-treated parasites as compared to DMSO. Relative abundance comparisons of total ion counts are means from two biological repeats collected in triplicate at each time of drug incubation. Error bars are standard deviations. Significant changes are adjusted *P* values of treatments as compared to DMSO. **P* < 0.05, ***P* < 0.01.

although ATQ (with a similar slow-acting phenotype) induces a significant metabolic signal indicative of its mode of action over the same duration of drug exposure (2.5 h). Future work using a longer incubation period might reveal unique signatures specific to this compound mode of action. Recently, *in vitro* selection for resistance and forward genetic screens have pointed to inhibition of protein trafficking as a possible mode of action of KAF156 and other IZPs (55), so rapid/early metabolic changes might not be associated with mode of action.

The initial global metabolomic responses to DHA, Cpd 55, and NITD246 are immediate, unique, and dynamic

Fast-acting compounds may exert a parasite killing event in seconds or minutes with resulting metabolic profiles over time resulting from deregulated metabolic cascades which may or may not relate to a specific mode of action of the compounds. For example, the spiroindolone, KAE609, has been shown to lead to a rapid influx of sodium-disrupting parasite ion homeostasis within seconds of drug exposure (46, 56). DHA is also known to target immediately several parasite proteins simultaneously in a promiscuous targeting process which leads to parasite death as a result of a disruption in several biological pathways (57, 58). In such events, metabolic and biochemical perturbations in essential pathways that are directly or indirectly involved in the mode of action of the compounds should be quantifiable within minutes of drug exposure. To this end, we aimed to resolve the dynamic metabolic fingerprints of *P. falciparum* in response to the three fast-acting compounds studied here (DHA, Cpd 55, and NITD246) at $10 \times IC_{50}$ exposure for 30 min and 1 and 2 h. For all three compounds, significant changes to the global parasite metabolome were already observed after 30 min of drug exposure. Over the time course, the profile, extent, and rate of change were time dependent and unique to each drug. The extent of change, however, was broadly equivalent for all three drugs after 2 h. Of the $\sim 3,000$ mass features which were detected in each analysis by liquid chromatography-based mass spectrometry (LC-MS), 4.3%, 1.6%, and 4.6% changed significantly (>0.2 log₂ fold change relative to DMSO control, adjusted *P* value <0.05) at 30 min, which increased to 5.6%, 5.8%, and 5.2% at 1 h and 7.8%, 8.1%, and 7.9% at 2 h for DHA, NITD246, and Cpd 55, respectively. Analysis of the volcano plots (Fig. 6) revealed that DHA elicits a stronger general downregulation of impacted metabolites after 30 min, although the magnitude of change converges toward those of NITD246 after 1 and 2 h. The global metabolomic response to Cpd 55 revealed differences compared to DHA and NITD246 at all time points, displaying lower magnitude fold changes symmetrically distributed around zero (Fig. 6). A unique, unvarying cluster of metabolites, possibly drug-related adducts, could be detected across the three time points (circled in red) in the Cpd 55 global metabolome. Overall, these global metabolome profiles indicate that, in spite of displaying a similar fast-killing rate and a signature impact on hemoglobin catabolism, additional discriminating features are already visible by 30 min of drug incubation and could point to as yet unknown drug-specific, parasite kill events.

NITD246-induced perturbation of choline, pyrimidine, and purine metabolites occurs shortly after compound administration

Our initial analyses established that NITD246 significantly perturbed metabolites in the pyrimidine, purine nucleotide, and choline biosynthetic pathways after 2.5 h of drug incubation (Fig. 3 and S2). Analysis of the early time-resolved profiles of these metabolites permitted discrimination between a progressive and dynamic response or an immediate metabolic shock response. From these analyses, it was evident that NITD246 induced a gradual accumulation of choline-related metabolites (Fig. 7A) that becomes visible at the 1- and 2-h time points. Interestingly, DHA elicits a similar choline response profile (Fig. S3A) which may indicate a common consequence to primary target inhibition by both compounds. By contrast, Cpd 55 does not alter choline homeostasis (Fig. 7A), further suggesting that the metabolic consequences of DHA and NITD246 exposure in malaria parasites overlap, while Cpd 55 acts via a different mode of action. A similar trend was observed for pyrimidine- and purine nucleotide-related metabolites that gradually decrease over 2 h of NITD246 drug incubation but remain unchanged in Cpd 55 (Fig. 7B to F). Uniquely, orotate pools sharply accumulated in NITD246-treated parasites after 30 min of drug incubation but rapidly declined thereafter to significantly lower levels after 2 h (Fig. 7B). This could be a result of preferential inhibition of the orotate phosphoribosyltransferase enzyme in the pyrimidine pathway during the initial assault on parasite ion homeostasis, which would lead to accumulation of orotate that returns to normal levels as other enzymes of the pathway respond to the perturbation.

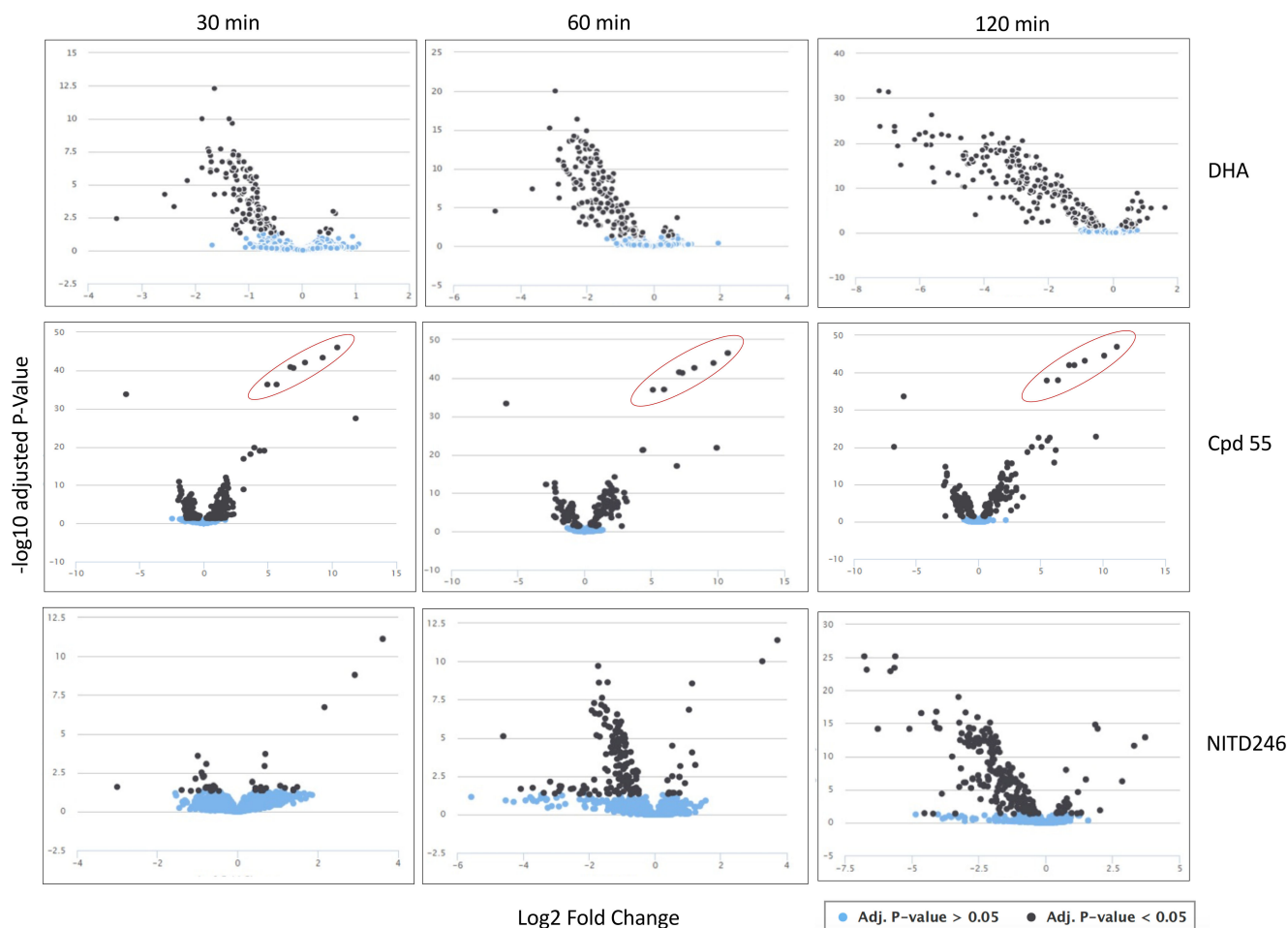


FIG 6 Global volcano plots of all detected mass features in DHA, Cpd 55 and NITD246 treatments according to their fold change relative to DMSO treatments. Significant features are represented as black dots, while non-significant features are in light blue. $n = 2$ with three replicates at each biological repeat. Red circled metabolites for Cpd 55 are potential drug-related mass features.

DHA did not induce any significant alteration in either purine nucleotides or metabolites of the pyrimidine biosynthesis pathway during the 2-h time period (Fig. S3B through F). Even though pyrimidine metabolite profiles were previously reported to change following exposure to DHA ($10 \times \text{IC}_{50}$, significant changes at 4 and 6 h) (24), the observed absence of the pyrimidine profile with DHA in this study could be due to the shorter duration of drug exposure.

Time-dependent changes in peptide response for NITD246, DHA, and Cpd 55

We also analyzed the dynamic peptide response in NITD246, DHA, and Cpd 55 treatments over the 0.5, 1.0, and 2.0 h of drug incubation. Analysis of the global peptide response in the three drug treatments revealed that this response is already visible at 30 min of drug incubation and becomes more pronounced at 1 and 2 h, respectively (Fig. 8A; Table S4). Moreover, even though the global peptide responses appear similar across the three compounds, Cpd 55 elicits a unique and early peptide response as compared to DHA and NITD246, which suggests a unique targeting of the parasite's hemoglobin catabolism by this class of compound that does not directly or indirectly impact other biochemical pathways over the time courses studied. Indeed, supervised clustering of the global peptidomes in these treatments by principal component analysis (PCA) revealed that at both time points, DHA and NITD246 peptide response clustered closer together than Cpd 55 or DMSO in the first and second principal components (Fig. 8B).

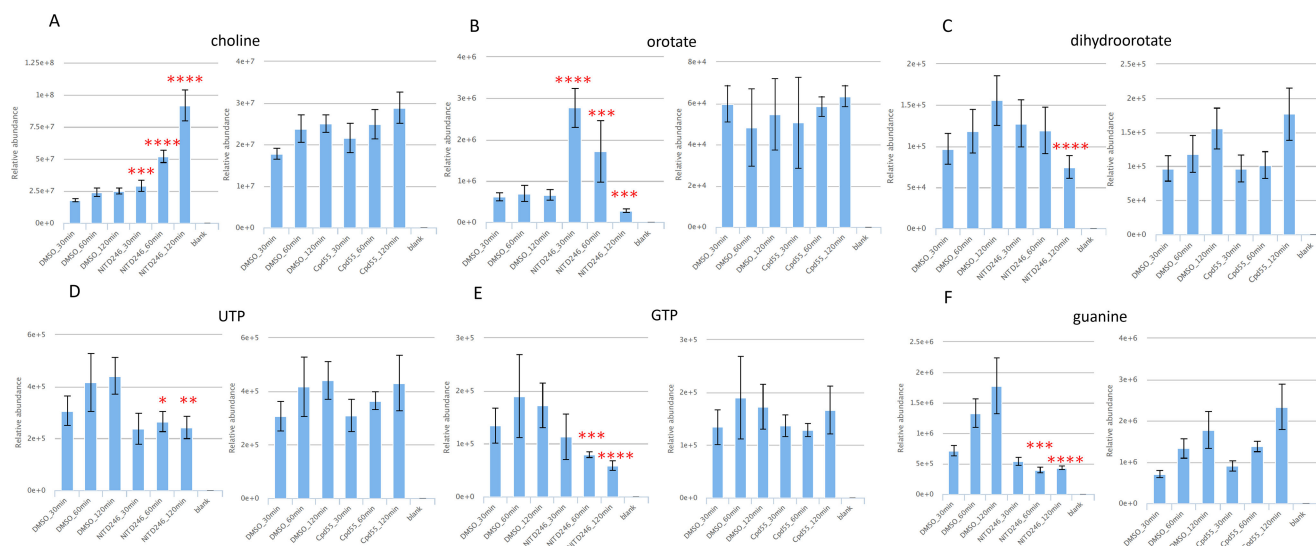


FIG 7 Time course comparisons of choline, pyrimidine, and purine metabolites in DHA, NITD246, and Cpd 55 parasite treatments. Relative abundance of choline (A), selected indicated pyrimidine (B through D), and purine (E and F) metabolites. Comparisons of total ion counts are means from two biological repeats collected in triplicate at each time of drug incubation. Error bars are standard deviations. Significant changes are adjusted P values of treatments as compared to DMSO for each individual time point. * $P < 0.05$, ** $P < 0.01$, *** $P < 0.001$, **** $P < 0.0001$.

Finally, some of the potentially hemoglobin-derived peptides such Trp-Gly showed a time-dependent decline in NITD246 and Cpd 55 treatments (Fig. 8C), further suggestive of a global decline in parasite hemoglobin catabolism as a consequence of drug treatment.

Conclusions

In conclusion, this study reports the metabolomic profile of a novel class of fast-acting compounds belonging to the ITD class, which suggests inhibition of hemoglobin catabolism as their possible mode of action or an essential secondary event that precedes their parasite killing mechanism. By direct comparison with DHA and spiroindolones, we show that fast-acting compounds elicit unique, but broadly similar, peptide profiles that are strikingly different from atovaquone and another slow-acting NITD compound, GNF179. These biochemical profiles can be used to predict the mode of action of similar fast-acting anti-malarial drugs and may also be used to identify fast-acting anti-malarial agents retrospectively if metabolomic based mode of action studies are incorporated in early stages of drug discovery (31, 32). Our approach to measure the time course of dynamic change of metabolome profiles shortly after drug administration may also help in differentiating fast-acting compounds based on peptide clusters if the specific mechanism of action is unknown, in the context of selecting partner drugs for combinations to mitigate the emergence of resistance.

MATERIALS AND METHODS

P. falciparum culture and maintenance

Two *P. falciparum* lines, 3D7 and a 3D7-derived luciferase reporter line (Judith Straimer, unpublished), were used for the experiments. The lines were cultured and maintained at 1%–5% parasitemia in fresh group O-positive red blood cells re-suspended to a 5% hematocrit in custom reconstituted RPMI 1640 complete media (Thermo Scientific) containing 0.23% sodium bicarbonate, 0.4% D-glucose, 0.005% hypoxanthine, 0.6% HEPES, 0.5% Albumax II, 0.03% L-glutamine, and 25-mg/L gentamicin. Culture flasks were gassed with a mixture of 1% O_2 , 5% CO_2 , and 94% N_2 and incubated at 37°C. For

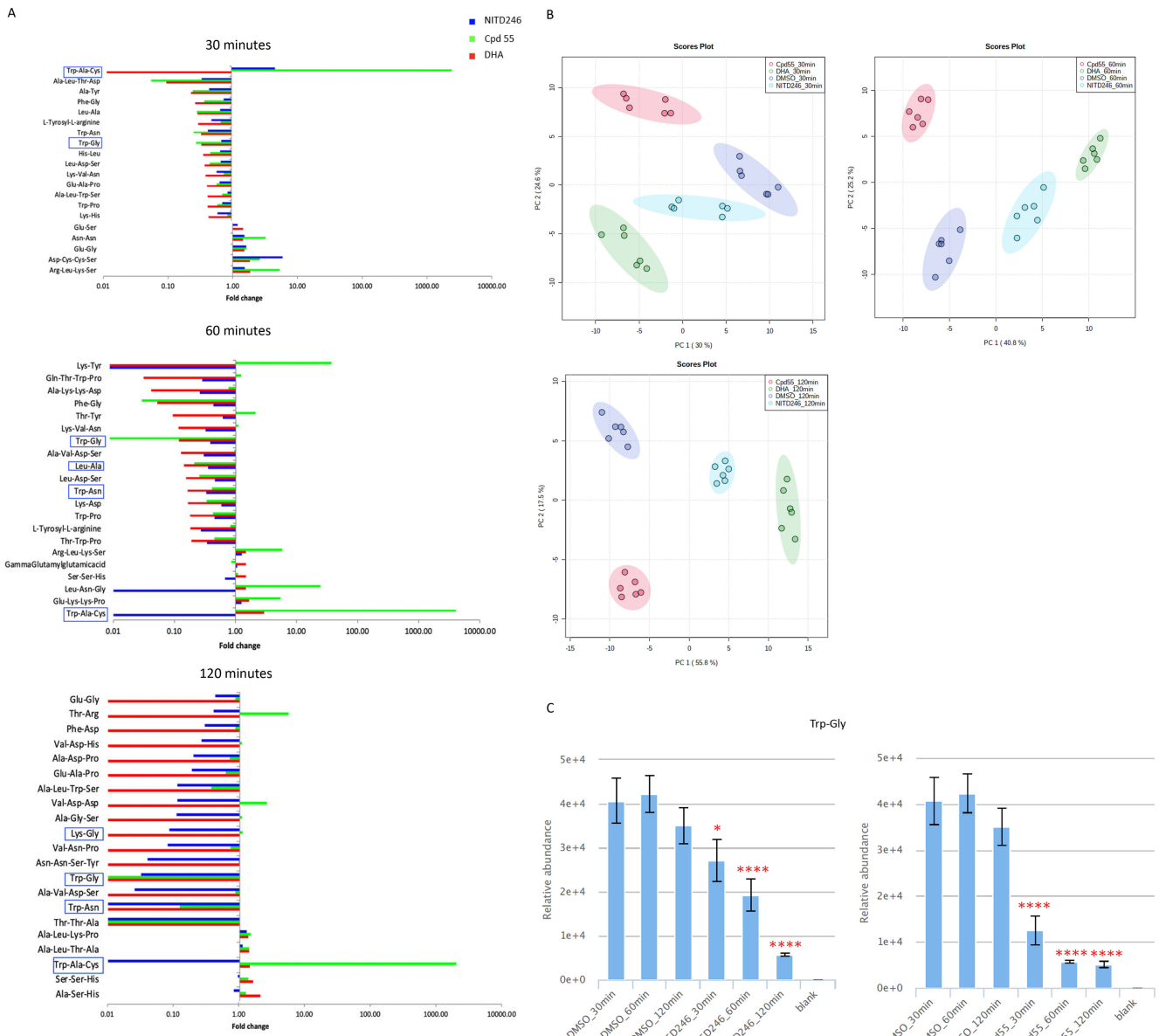


FIG 8 Time point resolution of global peptide responses in NITD246-, DHA-, and Cpd 55-treated parasites. (A) Global responses of top 20 significantly changed peptides upon treatment with DHA, NITD246, and Cpd 55 for 30 min and 1 and 2 h. Peptides with hemoglobin matching sequences as well as those that have been previously validated to be hemoglobin derived (24, 25) are highlighted. (B) PCA plots of the peptidomes of the three compounds after treatment for 30 min and 1 and 2 h. (C) Relative abundance of a potential hemoglobin-derived peptide Trp-Gly in DMSO vs the two indicated treatment compounds at the three time points. Fold changes and relative abundance comparisons are means from two biological repeats collected in triplicate at each time of drug incubation. PCA plots were carried out on log-transformed data in Metaboanalyst 3 (59). Ninety-five percent confidence intervals for each treatment group in the PCAs are highlighted with the indicated colors. Error bars are standard deviations. Significant changes are adjusted *P* values of treatments as compared to DMSO for each individual time point. **P* < 0.05, *****P* < 0.0001.

metabolomics experiments, parasites were scaled up to a 5%–7% parasitemia and sorbitol synchronized over two developmental cycles as previously described (60) to obtain parasites within a 3- to 6-h developmental window. In brief, cultures were pelleted by centrifugation at 1,600 rpm for 3 min and resuspended in a 10× volume of 5% sorbitol (Sigma), followed by incubation at 37°C for 10 min. Following incubation, the infected RBCs were pelleted as above and washed in 40 pellet volumes of complete media before placing the infected RBCs back in fresh media and subsequent incubation at 37°C.

Cultures were kept mycoplasma free, and mycoplasma contaminations were monitored weekly using the Mycoalert Luminescence Kit (Lonza).

***P. falciparum* SYBR green I assay for parasite growth inhibition**

Asynchronous stock cultures containing mainly ring stages were synchronized with 5% sorbitol as described above. Parasitemia was quantified in the synchronized cultures with drug assays performed when the parasitemia was between 1.5% and 5.0% with >90% rings. The stock culture was diluted to a hematocrit of 4.0% and 0.3% parasitemia in complete media following which 50 μ L was mixed with 50 μ L of serial diluted drugs/inhibitors in complete media pre-dispensed in black 96-well optical culture plates (Thermo Scientific) for a final hematocrit of 2%. Plates were gassed and incubated at 37°C for 72 h followed by freezing at -20°C for at least 24 h. The plate setup also included no drug controls as well as uninfected red cells at 2% hematocrit. After 72 h of incubation and at least overnight freezing at -20°C , the plates were thawed at room temperature for \sim 4 h. This was followed by addition of 100 μ L to each well of 1 \times SYBR Green I (Invitrogen) lysis buffer containing 20-mM Tris, 5-mM EDTA, 0.008% saponin, and 0.08% Triton X-100. Plate contents were mixed thoroughly by shaking at 700 rpm for 5 min and were incubated for 1 h at room temperature in the dark. After incubation, plates were read to quantify SYBR Green I fluorescence intensity in each well by a PHERAstar FSX microplate reader (BMG Labtech) or the CLARIOstar microplate reader (BMG Labtech) with excitation and emission wavelengths of 485 and 520 nm, respectively. To determine growth inhibition, background fluorescence intensity from uninfected red cells was subtracted first. Fluorescence intensity of no drug controls was then set to correspond to 100%, and subsequent intensity in the presence of drug/inhibitor was calculated accordingly. Dose-response curves and IC_{50} concentrations were plotted in GraphPad Prism v.7.

***P. falciparum* luciferase assay**

Metabolomic screens to characterize mode of action of compounds in malaria parasites rely on adequate exposure of parasites to the drugs for a good metabolic signal while avoiding overexposure, which can lead to death-related metabolic signatures (23). This is, however, difficult to quantify especially for fast-acting compounds which could potentially elicit metabolic signatures very early on in the parasite killing cascade. Previous studies have employed a concurrent monitoring of glycolytic intermediates over the 6-h course of drug exposure in midtrophozoites as a marker of parasite viability (25). Nevertheless, we aimed to determine the killing kinetics of our compounds of interest biochemically by monitoring luciferase expression in a 3D7 dual reporter line that stably expresses NanoLuc and luciferase (3D7 luc, unpublished) under the control of a constitutive calmodulin promoter. The line was generated by CRISPR-Cas9-mediated integration of the reporter cassette into the parasite genome at the elongase I locus. Synchronized trophozoites (\sim 30 h old) at 2% hematocrit and 2% parasitemia were incubated with the compounds at $10 \times \text{IC}_{50}$ for 0.5, 1.0, 1.5, 2.0, 2.5, 3.0, 3.5, 4.0, 5.0, and 6.0 h. Luciferase expression was quantified on a CLARIOstar microplate reader (BMG Labtech). Briefly, 100 μ L of the reconstituted Dual-Luciferase Reporter reagent (Promega) was mixed with 100- μ L parasite culture and incubated at room temperature in the dark for 15 min. Luciferase signal was quantified immediately after the incubation. Parasite viability was also monitored by microscopy analysis of methanol-fixed Giemsa-stained smears.

Magnetic purification of trophozoites

Drug induced metabolomic screens are mostly performed on 24- to 30-h-old trophozoites as they yield better metabolic signatures as well as less variability (23). To enrich for \sim 24- to 30-h-old trophozoites, a magnetic separation was employed as previously described (61). Custom 3D printed magnet stands were assembled based on previously reported designs (61) and used to assemble a magnetic apparatus which was used to

enrich for mature trophozoites in conjunction with cell separation LD columns (Miltenyi Biotech). Briefly, synchronized cultures at 5%–7% parasitemia (~24 to 30 h old) were re-suspended to 8% hematocrit following which 5 mL was loaded into the LD columns on the magnetic stands and allowed to flow through. Uninfected and early-stage parasites were washed off by loading the LD column with 5 mL of clean complete media, which allows for removal of all unbound RBCs. Bound parasites were then eluted in 5 mL of fresh complete media after removal of the LD columns from the magnetic stands. Eluted parasites were pooled into a single falcon tube from which cell counts (hemocytometer counting) were performed and adjusted to a concentration of $\sim 1 \times 10^8$ cells/mL. Purified parasites, containing >90% purified trophozoites, were allowed to recover for ~1 h at 37°C at ~0.5% hematocrit before the start of experiments. Further quality and purity of the enriched trophozoites were assessed by microscopy analysis of methanol-fixed Giemsa-stained smears.

Metabolite sample preparation

Magnetically purified trophozoites as described above were exposed to DHA, NITD246, and inactive analog (NITD246i); GNF179; Cpd 9 and inactive analog Cpd 9_ia; Cpd 55 and inactive analog Cpd 55_ia at $10 \times IC_{50}$. ATQ was used as a positive control while DMSO (0.1%) was used in untreated controls. 1 mL of purified trophozoites (1×10^8 cells) was mixed with 4 mL of complete media containing spiroindolones, KAF156, ITDs, and ATQ at $10 \times IC_{50}$ in six-well plates for 2.5 h initially. The concentration used and the time of exposure were based on our time kill kinetics of these compounds as well as previously validated drug concentration and corresponding time points which are known to achieve a better metabolic signal resolution (23–25). To resolve the metabolic profiles of fast-acting compounds at earlier time points, a similar approach as described above was used for DHA, NITD246, and Cpd 55 albeit with a dynamic drug exposure for 0.5, 1.0, and 2.0 h. Incubations at all time points were performed in triplicate over two biological repeats. After drug incubation, 4 mL of media was aspirated from the six-well plates, and cells were resuspended in 1-mL volume and centrifuged to pellet the cells. Metabolism was immediately quenched by aspirating the supernatant and resuspending the cells in ice-cold $1 \times$ PBS. All experiments were performed on ice onward.

Metabolite extraction

A mixture of water, methanol, and chloroform (1:3:1) was used for metabolite extraction to allow for complimentary coverage of both polar and non-polar metabolites as previously described (62). The chilled suspension of cells was centrifuged at 8,500 *g* for 30 s at 4°C. After removing the supernatant, the cells were further washed by re-suspending in fresh 500 μ L of ice-cold $1 \times$ PBS, and the supernatant was removed again. Cell pellets were then re-suspended in 200 μ L of ice-cold chloroform/methanol/water in a 1:3:1 ratio. After vigorously shaking for 1 h in the cold room or chilled shaker at 4°C, the samples were sonicated for 2 min in ice-cold water and centrifuged at 15,300 *g* for 5 min at 4°C. The supernatant (~180 μ L) was transferred to 2-mL clean screw capped tubes for LC-MS analysis. Pooled sample controls were also prepared during this time for quality control during the LC-MS processing. An extraction solvent blank was also included as part of the internal controls. Samples were kept at -80°C until processed.

LC-MS metabolomics analysis

Untargeted LC-MS sample processing was carried out at the University of Glasgow Polyomics facility on a hydrophilic interaction liquid chromatography (pHILIC) on a Dionex UltiMate 3000 RSLC system (Thermo Fisher Scientific) using a ZIC-pHILIC column (150 mm [length] \times 4.6 mm [diameter], 5- μ m [bead size] column) coupled to a Thermo Orbitrap Q-Exactive mass spectrometer (Thermo Fisher Scientific). Ten microliters of the sample maintained on a 5°C auto-sampler was injected on a column that was maintained at 30°C. Samples were eluted on a linear gradient, starting with 20% A and 80% B for

15 min, followed by a 2 min wash with 95% A and 5% B, and 8-min re-equilibration with 20% A and 80% B, where solvent A is 20-mM ammonium carbonate in water, while solvent B is acetonitrile. The LC-MS method was based on previously published protocols (63). Mass spectrometry was operated in polarity switching mode at a resolution of 70,000, 10^6 cts automatic gain control (AGC) target, spray voltages +3.8 and -3.8 kV, capillary temperature of 320°C, heater temperature of 150°C, sheath gas flow rate of 40 a.u., auxiliary gas flow rate of 5 a.u., sweep gas flow rate of 5 a.u., and a full scan mass window of 70–1050 m/z. m/z 83.0604, 149.0233, and 445.1200 were used as lock masses in the positive mode, while m/z 89.0244 was used as a lock mass in the negative mode.

Mass spectrometry fragmentation

Samples were also subjected to a fragmentation mass spectrometry analysis (tandem LC-MS) to allow for additional structural information on detected mass features. Fragmentation of the samples was carried out in either the positive or negative ionization modes or both using duty cycles (one full scan event and one top 5 or top 10 fragmentation events) as previously described (64).

Data acquisition

Control runs consisting of blank runs and standardized internal controls were run in accordance with standard procedures at the Glasgow Polyomics to monitor the performance of the mass spectrometer in terms of chromatography and mass intensities. A mixture of standards containing 150 reference compounds available from Glasgow Polyomics was also run to assess the quality of the mass spectrometer and to aid in metabolite annotation and identification (63). Pooled samples containing fractional representation of samples were run prior to and across the batch every sixth sample to monitor the stability and quality of the LC-MS run, whereas the actual samples were run in a randomized manner to minimize batch effects. Thermo Xcalibur Tune software was used for instrument control and data acquisition. After acquisition, all raw files were converted into mzXML format, separating positive and negative ionization mode spectra into two different mzXML files using the command line version of MSconvert (ProteoWizard).

Data processing, analysis, and metabolite identification

Data files in mzXML format were processed using an Excel interface, IDEOM (65), which is based on XCMS and mzmatch R tools that allow raw peak extraction, noise-filtering, gap-filling, and peak annotations (66, 67). mzXML files were also processed using PiMP, a web-based Glasgow Polyomics metabolomics data processing pipeline (68) that is also based on XCMS and mzmatch R tools (66, 67) but allows for easy and multiple sample comparisons across experimental conditions. Volcano plots and principal component analysis were visualized and plotted both in IDEOM, PiMP, and Metaboanalyst 3 (59). Metabolite changes across different conditions and time points were plotted as fold changes or log₂ fold changes. Identification of metabolites was based on fragmentation spectra, retention time and mass compared to authentic standards as previously outlined by the Metabolomics Standards Initiative (MSI) (69). Metabolites that matched an authentic standard with or without a fragmentation spectrum were classified as identified (MSI level 1). Metabolites that did not match any authentic standards but had spectral similarities with spectral libraries (<https://www.genome.jp/kegg/pathway.html>) were classified as putatively annotated and were analyzed further based on fragmentation spectra, if available. All raw data and experimental metadata are available in the Metabolights data repository (accession number: [MTBL56580](https://www.ebi.ac.uk/metabolights/)).

ACKNOWLEDGMENTS

This work was supported by grants from the Wellcome Trust to A.P.W. (083811/Z/07/Z and 107046/Z/15/Z). M.P.B. is funded by a Wellcome Trust core grant to the Wellcome

Centre for Integrative Parasitology (104111/Z/14/Z). N.V.S. was funded by a Commonwealth Doctoral Studentship (MWCS-2017-789) and the Novartis Global Health Fellowships.

AUTHOR AFFILIATIONS

¹Institute of Infection, Immunity and Inflammation, Wellcome Centre for Integrative Parasitology, University of Glasgow, Glasgow, United Kingdom

²Novartis Institute for Tropical Diseases, Emeryville, California, USA

AUTHOR ORCID*s*

Nelson V. Simwela  <http://orcid.org/0009-0009-5607-9479>

Andrew P. Waters  <http://orcid.org/0000-0001-8900-2982>

FUNDING

Funder	Grant(s)	Author(s)
Wellcome Trust (WT)	107046/Z/15/Z, 083811/Z/07/Z, 104111/Z/14/Z	Andrew P. Waters Michael P. Barrett
Novartis AG Novartis Institutes for BioMedical Research (NIBR)		Nelson V. Simwela
Commonwealth Scholarship Commission (CSC)	MWCS-2017-789	Nelson V. Simwela

AUTHOR CONTRIBUTIONS

Nelson V. Simwela, Conceptualization, Data curation, Formal analysis, Investigation, Methodology, Writing – original draft, Writing – review and editing | W. Armand Guiguemde, Conceptualization, Data curation, Formal analysis, Visualization, Writing – review and editing | Judith Straimer, Data curation, Formal analysis, Investigation, Writing – review and editing | Clement Regnault, Investigation, Methodology, Writing – review and editing | Fumiaki Yokokawa, Investigation, Methodology, Writing – review and editing | Benjamin Taft, Investigation, Methodology, Writing – review and editing | Thierry T. Diagana, Conceptualization, Data curation, Funding acquisition, Investigation, Supervision, Writing – review and editing | Michael P. Barrett, Conceptualization, Data curation, Formal analysis, Investigation, Supervision, Writing – original draft, Writing – review and editing.

ADDITIONAL FILES

The following material is available [online](#).

Supplemental Material

Supplemental figures (Spectrum03976-22-s0001.pdf). Fig. S1 to S3.

Table S1 (Spectrum03976-22-s0002.xlsx). A global peptide response in NITD246-treated parasites as compared to DMSO at 2.5 h.

Table S2 (Spectrum03976-22-s0003.xlsx). A global peptide response in Cpd 9-treated parasites as compared to DMSO at 2.5 h.

Table S3 (Spectrum03976-22-s0004.xlsx). A global peptide response in Cpd 55-treated parasites as compared to DMSO at 2.5 h.

Table S4 (Spectrum03976-22-s0005.xlsx). A global peptide response in NITD246-, Cpd 55-, and DHA-treated parasites as compared to DMSO at 30, 60, and 120 min.

REFERENCES

- WHO. 2018. World malaria report. World Health Organisation, Geneva, Switzerland.
- Hemingway J, Shretta R, Wells TNC, Bell D, Djimé AA, Achee N, Qi G. 2016. Tools and strategies for malaria control and elimination: what do we need to achieve a grand convergence in malaria? *PLoS Biol* 14:e1002380. <https://doi.org/10.1371/journal.pbio.1002380>
- Dondorp AM, Nosten F, Yi P, Das D, Phyto AP, Tarning J, Lwin KM, Ariey F, Hanpithakpong W, Lee SJ, Ringwald P, Silamut K, Imwong M, Chotivanich K, Lim P, Herdman T, An SS, Yeung S, Singhasivanon P, Day NPJ, Linddegardh N, Socheat D, White NJ. 2009. Artemisinin resistance in *Plasmodium falciparum* malaria. *N Engl J Med* 361:455–467. <https://doi.org/10.1056/NEJMoa0808859>
- Ashley EA, Dhorda M, Fairhurst RM, Amaratunga C, Lim P, Suon S, Sreng S, Anderson JM, Mao S, Sam B, Sopha C, Chuur CM, Nguon C, Sovannaroth S, Pukrittayakamee S, Jittamala P, Chotivanich K, Chutasmit K, Suchatsoonthorn C, Runcharoen R, Hien TT, Thuy-Nhien NT, Thanh NV, Phu NH, Htut Y, Han K-T, Aye KH, Mokuolu OA, Olaosebikan RR, Folaranmi OO, Mayxay M, Khanthavong M, Hongvanthong B, Newton PN, Onyamboko MA, Fanello CI, Tshetu AK, Mishra N, Valecha N, Phyto AP, Nosten F, Yi P, Tripura R, Borrmann S, Bashraheil M, Peshu J, Faiz MA, Ghose A, Hossain MA, Samad R, Rahman MR, Hasan MM, Islam A, Miotto O, Amato R, MacInnis B, Stalker J, Kwiatkowski DP, Bozdech Z, Jeeyapant A, Cheah PY, Sakulthawet T, Chalk J, Intharabut B, Silamut K, Lee SJ, Vihokhern B, Kunasol C, Imwong M, Tarning J, Taylor WJ, Yeung S, Woodrow CJ, Flegg JA, Das D, Smith J, Venkatesan M, Plowe CV, Stepniewska K, Guerin PJ, Dondorp AM, Day NP, White NJ, Tracking Resistance to Artemisinin Collaboration (TRAC). 2014. Spread of artemisinin resistance in *Plasmodium falciparum* malaria. *N Engl J Med* 371:411–423. <https://doi.org/10.1056/NEJMoa1314981>
- Ménard D, Khim N, Beghain J, Adegnikaa AA, Shafiu-Alam M, Amodu O, Rahim-Awab G, Barnadas C, Berry A, Boum Y, Bustos MD, Cao J, Chen J-H, Collet L, Cui L, Thakur G-D, Dieye A, Djallé D, Dorkenoo MA, Eboombou-Moukoko CE, Espino F-E-CJ, Fandeur T, Ferreira-da-Cruz M-F, Fola AA, Fuehrer H-P, Hassan AM, Herrera S, Hongvanthong B, Houzé S, Ibrahim ML, Jahirul-Karim M, Jiang L, Kano S, Ali-Khan W, Khanthavong M, Kremsner PG, Lacerda M, Leang R, Leelawong M, Li M, Lin K, Mazarati J-B, Ménard S, Morlais I, Muhindo-Mavoko H, Musset L, Na-Bangchang K, Nambozi M, Niaré K, Noedl H, Ouedraogo J-B, Pillai DR, Pradines B, Quang-Phuc B, Ramharther M, Randrianarivoelosia M, Sattabongkot J, Sheikh-Omar A, Silué KD, Sirima SB, Sutherland C, Syafruddin D, Tahar R, Tang L-H, Touré OA, Tshibangu-wa-Tshibangu P, Vigan-Womas I, Warsame M, Wini L, Zakeri S, Kim S, Eam R, Berne L, Khean C, Chy S, Ken M, Loch K, Canier L, Duru V, Legrand E, Barale J-C, Stokes B, Straimer J, Witkowski B, Fidock DA, Rogier C, Ringwald P, Ariey F, Mercereau-Puijalón O, KARMA Consortium. 2016. A worldwide map of *Plasmodium falciparum* K13-propeller polymorphisms. *N Engl J Med* 374:2453–2464. <https://doi.org/10.1056/NEJMoa1513137>
- Balikagala B, Fukuda N, Ikeda M, Katuro OT, Tachibana SI, Yamauchi M, Opio W, Emoto S, Anywar DA, Kimura E, Palacpac NMQ, Odongo-Aginya E, Ogwang M, Horii T, Mita T. 2021. Evidence of artemisinin-resistant malaria in Africa. *N Engl J Med* 385:1163–1171. <https://doi.org/10.1056/NEJMoa2101746>
- Hamilton WL, Amato R, van der Pluijm RW, Jacob CG, Quang HH, Thuy-Nhien NT, Hien TT, Hongvanthong B, Chindavongsa K, Mayxay M, Huy R, Leang R, Huch C, Dysoley L, Amaratunga C, Suon S, Fairhurst RM, Tripura R, Peto TJ, Sovann Y, Jittamala P, Hanboonkunupakarn B, Pukrittayakamee S, Chau NH, Imwong M, Dhorda M, Vongpromek R, Chan XHS, Maude RJ, Pearson RD, Nguyen T, Rockett K, Drury E, Gonçalves S, White NJ, Day NP, Kwiatkowski DP, Dondorp AM, Miotto O. 2019. Evolution and expansion of multidrug-resistant malaria in Southeast Asia: a genomic epidemiology study. *Lancet Infect Dis* 19:943–951. [https://doi.org/10.1016/S1473-3099\(19\)30392-5](https://doi.org/10.1016/S1473-3099(19)30392-5)
- van der Pluijm RW, Imwong M, Chau NH, Hoa NT, Thuy-Nhien NT, Thanh NV, Jittamala P, Hanboonkunupakarn B, Chutasmit K, Saelow C, Runjarern R, Kaewmok W, Tripura R, Peto TJ, Yok S, Suon S, Sreng S, Mao S, Oun S, Yen S, Amaratunga C, Lek D, Huy R, Dhorda M, Chotivanich K, Ashley EA, Mukaka M, Waithira N, Cheah PY, Maude RJ, Amato R, Pearson RD, Gonçalves S, Jacob CG, Hamilton WL, Fairhurst RM, Tarning J, Winterberg M, Kwiatkowski DP, Pukrittayakamee S, Hien TT, Day NP, Miotto O, White NJ, Dondorp AM. 2019. Determinants of dihydroartemisinin-piperaquine treatment failure in *Plasmodium falciparum* malaria in Cambodia, Thailand, and Vietnam: a prospective clinical, pharmacological, and genetic study. *Lancet Infect Dis* 19:952–961. [https://doi.org/10.1016/S1473-3099\(19\)30391-3](https://doi.org/10.1016/S1473-3099(19)30391-3)
- Guiguemde WA, Shelat AA, Bouck D, Duffy S, Crowther GJ, Davis PH, Smithson DC, Connelly M, Clark J, Zhu F, Jiménez-Díaz MB, Martínez MS, Wilson EB, Tripathi AK, Gut J, Sharlow ER, Bathurst I, El Mazouni F, Fowle JW, Forquer I, McGinley PL, Castro S, Angulo-Barturen I, Ferrer S, Rosenthal PJ, Derisi JL, Sullivan DJ, Lazo JS, Roos DS, Riscoe MK, Phillips MA, Rathod PK, Van Voorhis WC, Avery VM, Guy RK. 2010. Chemical genetics of *Plasmodium falciparum*. *Nature* 465:311–315. <https://doi.org/10.1038/nature09099>
- Van Voorhis WC, Adams JH, Adelfio R, Ahlyong V, Akabas MH, Alano P, Alday A, Alemán Resto Y, Alsibae A, Alzualde A, Andrews KT, Avery SQ, Avery VM, Ayong L, Baker M, Baker S, Ben Mamoun C, Bhatia S, Bickle Q, Bounaadja L, Bowling T, Bosch J, Boucher LE, Boyom FF, Brea J, Brennan M, Burton A, Caffrey CR, Camarda G, Carrasquilla M, Carter D, Belen Cassera M, Chih-Chien Cheng K, Chindaudomsate W, Chubb A, Colon BL, Colón-López DD, Corbett Y, Crowther GJ, Cowan N, D'Alessandro S, Le Dang N, Delves M, DeRisi JL, Du AY, Duffy S, Abd El-Salam El-Sayed S, Ferdig MT, Fernández Robledo JA, Fidock DA, Florent I, Fokou PVT, Galstian A, Gamo FJ, Gokool S, Gold B, Golub T, Goldgof GM, Guha R, Guiguemde WA, Gural N, Guy RK, Hansen MAE, Hanson KK, Hemphill A, Hoof van Huijsduijn R, Horii T, Horrocks P, Hughes TB, Huston C, Igarashi I, Ingram-Sieber K, Itoe MA, Jadhav A, Naranuntarat Jensen A, Jensen LT, Jiang RHY, Kaiser A, Keiser J, Ketan S, Kicks S, Kim S, Kirk K, Kumar VP, Kyle DE, Lafuente MJ, Landfear S, Lee N, Lee S, Lehane AM, Li F, Little D, Liu L, Llinás M, Loza MI, Lubar A, Lucantoni L, Lucet I, Maes L, Mancama D, Mansour NR, March S, McGowan S, Medina Vera I, Meister S, Mercer L, Mestres J, Mfopa AN, Misra RN, Moon S, Moore JP, Morais Rodrigues da Costa F, Müller J, Muriana A, Nakazawa Hewitt S, Nare B, Nathan C, Narraido N, Nawaratna S, Ojo KK, Ortiz D, Panic G, Papadatos G, Parapini S, Patra K, Pham N, Prasad S, Plouffe DM, Poulsen S-A, Pradhan A, Quevedo C, Quinn RJ, Rice CA, Abdo Rizk M, Ruecker A, St Onge R, Salgado Ferreira R, Samra J, Robinett NG, Schlecht U, Schmitt M, Silva Villela F, Silvestrini F, Sinden R, Smith DA, Soldati S, Spitzmüller A, Stamm SM, Sullivan DJ, Sullivan W, Suresh S, Suzuki BM, Suzuki Y, Swamidass SJ, Taramelli D, Tchokouaha LRY, Theron A, Thomas D, Tonissen KF, Townson S, Tripathi AK, Trofimov V, Udenze KO, Ullah I, Vallieres C, Vigil E, Vinetz JM, Voong Vinh P, Vu H, Watanabe N-A, Weatherby K, White PM, Wilks AF, Winzeler EA, Wojcik E, Wree M, Wu W, Yokoyama N, Zollo PHA, Aba N, Blasco B, Burrows J, Laleu B, Leroy D, Spangenberg T, Wells T, Willis PA. 2016. Open source drug discovery with the malaria box compound collection for neglected diseases and beyond. *PLoS Pathog* 12:e1005763. <https://doi.org/10.1371/journal.ppat.1005763>
- Gamo F-J, Sanz LM, Vidal J, de Cozar C, Alvarez E, Lavandera J-L, Vanderwall DE, Green DVS, Kumar V, Hasan S, Brown JR, Peishoff CE, Cardon LR, Garcia-Bustos JF. 2010. Thousands of chemical starting points for antimalarial lead identification. *Nature* 465:305–310. <https://doi.org/10.1038/nature09107>
- Müller IB, Hyde JE. 2010. Antimalarial drugs: modes of action and mechanisms of parasite resistance. *Future Microbiol* 5:1857–1873. <https://doi.org/10.2217/fmb.10.136>
- Creek DJ, Barrett MP. 2014. Determination of antiprotozoal drug mechanisms by metabolomics approaches. *Parasitology* 141:83–92. <https://doi.org/10.1017/S0031182013000814>
- Fidock DA, Nomura T, Talley AK, Cooper RA, Dzekunov SM, Ferdig MT, Ursos LM, Sidhu AB, Naudé B, Deitsch KW, Su XZ, Wootton JC, Roepe PD, Welles TE. 2000. Mutations in the *P. falciparum* digestive vacuole transmembrane protein PfCRT and evidence for their role in chloroquine resistance. *Mol Cell* 6:861–871. [https://doi.org/10.1016/S1097-2765\(05\)00077-8](https://doi.org/10.1016/S1097-2765(05)00077-8)
- Korsunczyk M, Chen N, Kotecka B, Saul A, Rieckmann K, Cheng Q. 2000. Mutations in *Plasmodium falciparum* cytochrome b that are associated with atovaquone resistance are located at a putative drug-binding site. *Antimicrob Agents Chemother* 44:2100–2108. <https://doi.org/10.1128/AAC.44.8.2100-2108.2000>
- Thaithong S, Chan SW, Songsomboon S, Wilairat P, Seesod N, Sueblinwong T, Goman M, Ridley R, Beale G. 1992. Pyrimethamine resistant mutations in *Plasmodium falciparum*. *Mol Biochem Parasitol* 52:149–157. [https://doi.org/10.1016/0166-6851\(92\)90047-n](https://doi.org/10.1016/0166-6851(92)90047-n)

17. McNamara CW, Lee MC, Lim CS, Lim SH, Roland J, Simon O, Yeung BK, Chatterjee AK, McCormack SL, Manary MJ, Zeeman A-M, DeChering KJ, Kumar TS, Henrich PP, Gagaring K, Ibanez M, Kato N, Kuhen KL, Fischli C, Nagle A, Rottmann M, Plouffe DM, Bursulaya B, Meister S, Rameh L, Trappe J, Haasen D, Timmerman M, Sauerwein RW, Suwanarusk R, Russell B, Renia L, Nosten F, Tully DC, Kocken CH, Glynne RJ, Bodenreider C, Fidock DA, Diagona TT, Winzeler EA. 2013. Targeting *Plasmodium* P(4)K to eliminate malaria. *Nature* 504:248–253. <https://doi.org/10.1038/nature12782>
18. Baragaña B, Hallyburton I, Lee MCS, Norcross NR, Grimaldi R, Otto TD, Proto WR, Blagborough AM, Meister S, Wirjanata G, Ruecker A, Upton LM, Abraham TS, Almeida MJ, Pradhan A, Porzelle A, Luksch T, Martínez MS, Luksch T, Bolscher JM, Woodland A, Norval S, Zuccotto F, Thomas J, Simeons F, Stojanovski L, Osuna-Cabello M, Brock PM, Churcher TS, Sala KA, Zakutansky SE, Jiménez-Díaz MB, Sanz LM, Riley J, Basak R, Campbell M, Avery VM, Sauerwein RW, DeChering KJ, Noviyanti R, Campo B, Frearson JA, Angulo-Barturen I, Ferrer-Bazaga S, Gamo FJ, Wyatt PG, Leroy D, Siegl P, Delves MJ, Kyle DE, Wittlin S, Marfurt J, Price RN, Sinden RE, Winzeler EA, Charman SA, Bebrevska L, Gray DW, Campbell S, Fairlamb AH, Willis PA, Rayner JC, Fidock DA, Read KD, Gilbert IH. 2015. A novel multiple-stage antimalarial agent that inhibits protein synthesis. *Nature* 522:315–320. <https://doi.org/10.1038/nature14451>
19. Lukens AK, Ross LS, Heidebrecht R, Javier Gamo F, Lafuente-Monasterio MJ, Booker ML, Hartl DL, Wiegand RC, Wirth DF. 2014. Harnessing evolutionary fitness in *Plasmodium falciparum* for drug discovery and suppressing resistance. *Proc Natl Acad Sci U S A* 111:799–804. <https://doi.org/10.1073/pnas.1320886110>
20. Herman JD, Rice DP, Ribacke U, Siltrera J, Deik AA, Moss EL, Broadbent KM, Neafsey DE, Desai MM, Clish CB, Mazitschek R, Wirth DF. 2014. A genomic and evolutionary approach reveals non-genetic drug resistance in malaria. *Genome Biol* 15:511. <https://doi.org/10.1186/PREACCEPT-1067113631444973>
21. Vincent IM, Ehmann DE, Mills SD, Perros M, Barrett MP. 2016. Untargeted metabolomics to ascertain antibiotic modes of action. *Antimicrob Agents Chemother* 60:2281–2291. <https://doi.org/10.1128/AAC.02109-15>
22. Zampieri M, Szappanos B, Buchieri MV, Trauner A, Piazza I, Picotti P, Gagneux S, Borrell S, Gicquel B, Lelievre J, Papp B, Sauer U. 2018. High-throughput metabolomic analysis predicts mode of action of uncharacterized antimicrobial compounds. *Sci Transl Med* 10:eal3973. <https://doi.org/10.1126/scitranslmed.aal3973>
23. Allman EL, Painter HJ, Samra J, Carrasquilla M, Llinás M. 2016. Metabolomic profiling of the malaria box reveals antimalarial target pathways. *Antimicrob Agents Chemother* 60:6635–6649. <https://doi.org/10.1128/AAC.01224-16>
24. Cobbold SA, Chua HH, Nijagal B, Creek DJ, Ralph SA, McConville MJ. 2016. Metabolic dysregulation induced in *Plasmodium falciparum* by dihydroartemisinin and other front-line antimalarial drugs. *J Infect Dis* 213:276–286. <https://doi.org/10.1093/infdis/jiv372>
25. Creek DJ, Chua HH, Cobbold SA, Nijagal B, MacRae JI, Dickerman BK, Gilson PR, Ralph SA, McConville MJ. 2016. Metabolomics-based screening of the malaria box reveals both novel and established mechanisms of action. *Antimicrob Agents Chemother* 60:6650–6663. <https://doi.org/10.1128/AAC.01226-16>
26. Kwon YK, Lu W, Melamud E, Khanam N, Bognar A, Rabinowitz JD. 2008. A domino effect in antifolate drug action in *Escherichia coli*. *Nat Chem Biol* 4:602–608. <https://doi.org/10.1038/nchembio.108>
27. van Brummelen AC, Olszewski KL, Wilinski D, Llinás M, Louw AI, Birkholtz L-M. 2009. Co-inhibition of *Plasmodium falciparum* S-adenosylmethionine decarboxylase/ornithine decarboxylase reveals perturbation-specific compensatory mechanisms by transcriptome, proteome, and metabolome analyses. *J Biol Chem* 284:4635–4646. <https://doi.org/10.1074/jbc.M807085200>
28. Biagini GA, Fisher N, Shone AE, Mubarak MA, Srivastava A, Hill A, Antoine T, Warman AJ, Davies J, Pidathala C, Amewu RK, Leung SC, Sharma R, Gibbons P, Hong DW, Pacorel B, Lawrenson AS, Charoensuthivarakul S, Taylor L, Berger O, Mbekeani A, Stocks PA, Nixon GL, Chadwick J, Hemingway J, Delves MJ, Sinden RE, Zeeman A-M, Kocken CHM, Berry NG, O'Neill PM, Ward SA. 2012. Generation of quinolone antimalarials targeting the *Plasmodium falciparum* mitochondrial respiratory chain for the treatment and prophylaxis of malaria. *Proc Natl Acad Sci U S A* 109:8298–8303. <https://doi.org/10.1073/pnas.1205651109>
29. Lewis IA, Wacker M, Olszewski KL, Cobbold SA, Baska KS, Tan A, Ferdig MT, Llinás M. 2014. Metabolic QTL analysis links chloroquine resistance in *Plasmodium falciparum* to impaired hemoglobin catabolism. *PLoS Genet* 10:e1004085. <https://doi.org/10.1371/journal.pgen.1004085>
30. Birrell GW, Challis MP, De Paoli A, Anderson D, Devine SM, Heffernan GD, Jacobus DP, Edstein MD, Siddiqui G, Creek DJ. 2020. Multi-omic characterization of the mode of action of a potent new antimalarial compound, JPC-3210, against *Plasmodium falciparum*. *Mol Cell Proteomics* 19:308–325. <https://doi.org/10.1074/mcp.RA119.001797>
31. Antonova-Koch Y, Meister S, Abraham M, Luth MR, Otilie S, Lukens AK, Sakata-Kato T, Vanaerschot M, Owen E, Jado JC, Maher SP, Calla J, Plouffe D, Zhong Y, Chen K, Chaumeau V, Conway AJ, McNamara CW, Ibanez M, Gagaring K, Serrano FN, Eribez K, Taggard CM, Cheung AL, Lincoln C, Ambachew B, Rouillier M, Siegel D, Nosten F, Kyle DE, Gamo FJ, Zhou Y, Llinás M, Fidock DA, Wirth DF, Burrows J, Campo B, Winzeler EA. 2018. Open-source discovery of chemical leads for next-generation chemoprotective antimalarials. *Science* 362:eaat9446. <https://doi.org/10.1126/science.aat9446>
32. Cowell AN, Istvan ES, Lukens AK, Gomez-Lorenzo MG, Vanaerschot M, Sakata-Kato T, Flannery EL, Magistrado P, Owen E, Abraham M, LaMonte G, Painter HJ, Williams RM, Franco V, Linares M, Arriaga I, Bopp S, Corey VC, Gnädig NF, Coburn-Flynn O, Reimer C, Gupta P, Murithi JM, Moura PA, Fuchs O, Sasaki E, Kim SW, Teng CH, Wang LT, Akidil A, Adjalley S, Willis PA, Siegel D, Tanaseichuk O, Zhong Y, Zhou Y, Llinás M, Otilie S, Gamo F-J, Lee MCS, Goldberg DE, Fidock DA, Wirth DF, Winzeler EA. 2018. Mapping the malaria parasite druggable genome by using *in vitro* evolution and chemogenomics. *Science* 359:191–199. <https://doi.org/10.1126/science.aan4472>
33. Taft BR, Yokokawa F, Kirrane T, Mata AC, Huang R, Blaquiére N, Waldron G, Zou B, Simon O, Vankadara S, Chan WL, Ding M, Sim S, Straimer J, Guiguemde A, Lakshminarayana SB, Jain JP, Bodenreider C, Thompson C, Lanshoef C, Shu W, Fang E, Qumber J, Chan K, Pei L, Chen YL, Schulz H, Lim J, Abbas SN, Ang X, Liu Y, Angulo-Barturen I, Jiménez-Díaz MB, Gamo FJ, Crespo-Fernandez B, Rosenthal PJ, Cooper RA, Tumwebaze P, Aguiar ACC, Campo B, Campbell S, Wagner J, Diagona TT, Sarko C. 2022. Discovery and preclinical pharmacology of INE963, a potent and fast-acting blood-stage antimalarial with a high barrier to resistance and potential for single-dose cures in uncomplicated malaria. *J Med Chem* 65:3798–3813. <https://doi.org/10.1021/acs.jmedchem.1c01995>
34. Rottmann M, McNamara C, Yeung BKS, Lee MCS, Zou B, Russell B, Seitz P, Plouffe DM, Dharia NV, Tan J, Cohen SB, Spencer KR, González-Páez GE, Lakshminarayana SB, Goh A, Suwanarusk R, Jegla T, Schmitt EK, Beck H-P, Brun R, Nosten F, Renia L, Dartois V, Keller TH, Fidock DA, Winzeler EA, Diagona TT. 2010. Spiroindolones, a potent compound class for the treatment of malaria. *Science* 329:1175–1180. <https://doi.org/10.1126/science.1193225>
35. Lim MY-X, LaMonte G, Lee MCS, Reimer C, Tan BH, Corey V, Tjahjadi BF, Chua A, Nachon M, Wintjens R, Gedeck P, Malleret B, Renia L, Bonamy GMC, Ho PC-L, Yeung BKS, Chow ED, Lim L, Fidock DA, Diagona TT, Winzeler EA, Bifani P. 2016. UDP-galactose and acetyl-CoA transporters as *Plasmodium* multidrug resistance genes. *Nat Microbiol* 1:16166. <https://doi.org/10.1038/nmicrobiol.2016.166>
36. Kuhen KL, Chatterjee AK, Rottmann M, Gagaring K, Borboa R, Buenviaje J, Chen Z, Francec C, Wu T, Nagle A, Barnes SW, Plouffe D, Lee MCS, Fidock DA, Graumans W, van de Vegte-Bolmer M, van Gemert GJ, Wirjanata G, Sebayang B, Marfurt J, Russell B, Suwanarusk R, Price RN, Nosten F, Tungtaeng A, Gettayacamin M, Sattabongkot J, Taylor J, Walker JR, Tully D, Patra KP, Flannery EL, Vinetz JM, Renia L, Sauerwein RW, Winzeler EA, Glynne RJ, Diagona TT. 2014. KAF156 is an antimalarial clinical candidate with potential for use in prophylaxis, treatment, and prevention of disease transmission. *Antimicrob Agents Chemother* 58:5060–5067. <https://doi.org/10.1128/AAC.02727-13>
37. Meister S, Plouffe DM, Kuhen KL, Bonamy GMC, Wu T, Barnes SW, Bopp SE, Borboa R, Bright AT, Che J, Cohen S, Dharia NV, Gagaring K, Gettayacamin M, Gordon P, Groessl T, Kato N, Lee MCS, McNamara CW, Fidock DA, Nagle A, Nam T, Richmond W, Roland J, Rottmann M, Zhou B, Froissard P, Glynne RJ, Mazier D, Sattabongkot J, Schultz PG, Tuntland T, Walker JR, Zhou Y, Chatterjee A, Diagona TT, Winzeler EA. 2011. Imaging of *Plasmodium* liver stages to drive next-generation antimalarial drug

- discovery. *Science* 334:1372–1377. <https://doi.org/10.1126/science.1211936>
38. Sanz LM, Crespo B, De-Cózar C, Ding XC, Llergo JL, Burrows JN, García-Bustos JF, Gamo F-J. 2012. *P. falciparum* *in vitro* killing rates allow to discriminate between different antimalarial mode-of-action. *PLoS One* 7:e30949. <https://doi.org/10.1371/journal.pone.0030949>
 39. White NJ, Pukrittayakamee S, Phyo AP, Rueangweerayut R, Nosten F, Jittamala P, Jeeyapant A, Jain JP, Lefèvre G, Li R, Magnusson B, Diagona TT, Leong FJ. 2014. Spiroindolone KAE609 for *falciparum* and *vivax* malaria. *N Engl J Med* 371:403–410. <https://doi.org/10.1056/NEJMoa1315860>
 40. Srivastava IK, Morrisey JM, Darrouzet E, Daldal F, Vaidya AB. 1999. Resistance mutations reveal the atovaquone-binding domain of cytochrome b in malaria parasites. *Mol Microbiol* 33:704–711. <https://doi.org/10.1046/j.1365-2958.1999.01515.x>
 41. Painter HJ, Morrisey JM, Mather MW, Vaidya AB. 2007. Specific role of mitochondrial electron transport in blood-stage *Plasmodium falciparum*. *Nature* 446:88–91. <https://doi.org/10.1038/nature05572>
 42. MacRae JI, Dixon MW, Dearnley MK, Chua HH, Chambers JM, Kenny S, Bottova I, Tilley L, McConville MJ. 2013. Mitochondrial metabolism of sexual and asexual blood stages of the malaria parasite *Plasmodium falciparum*. *BMC Biol* 11:67–67. <https://doi.org/10.1186/1741-7007-11-67>
 43. Cobbold SA, Vaughan AM, Lewis IA, Painter HJ, Camargo N, Perlman DH, Fishbaugher M, Healer J, Cowman AF, Kappe SHI, Llinás M. 2013. Kinetic flux profiling elucidates two independent acetyl-CoA biosynthetic pathways in *Plasmodium falciparum*. *J Biol Chem* 288:36338–36350. <https://doi.org/10.1074/jbc.M113.503557>
 44. Ke H, Lewis IA, Morrisey JM, McLean KJ, Ganesan SM, Painter HJ, Mather MW, Jacobs-Lorena M, Llinás M, Vaidya AB. 2015. Genetic investigation of tricarboxylic acid metabolism during the *Plasmodium falciparum* life cycle. *Cell Rep* 11:164–174. <https://doi.org/10.1016/j.celrep.2015.03.011>
 45. Schmitt EK, Ndayisaba G, Yeka A, Asante KP, Grobusch MP, Karita E, Mugerwa H, Asiimwe S, Oduro A, Fofana B, Doumbia S, Su G, Csermak Renner K, Venishetty VK, Sayyed S, Straimer J, Demin I, Barsainya S, Boulton C, Gandhi P. 2022. Efficacy of cipargamin (KAE609) in a randomized, phase II dose-escalation study in adults in sub-Saharan Africa with uncomplicated *Plasmodium falciparum* malaria. *Clin Infect Dis* 74:1831–1839. <https://doi.org/10.1093/cid/ciab716>
 46. Das S, Bhatnagar S, Morrisey JM, Daly TM, Burns JM, Coppens I, Vaidya AB. 2016. Na⁺ influx induced by new antimalarials causes rapid alterations in the cholesterol content and morphology of *Plasmodium falciparum*. *PLoS Pathog* 12:e1005647. <https://doi.org/10.1371/journal.ppat.1005647>
 47. Zhang R, Suwanarusk R, Malleret B, Cooke BM, Nosten F, Lau Y-L, Dao M, Lim CT, Renia L, Tan KSW, Russell B. 2016. A basis for rapid clearance of circulating ring-stage malaria parasites by the spiroindolone KAE609. *J Infect Dis* 213:100–104. <https://doi.org/10.1093/infdis/jiv358>
 48. Spillman NJ, Kirk K. 2015. The malaria parasite cation ATPase PfATP4 and its role in the mechanism of action of a new arsenal of antimalarial drugs. *Int J Parasitol Drugs Drug Resist* 5:149–162. <https://doi.org/10.1016/j.ijpddr.2015.07.001>
 49. Lehane AM, Ridgway MC, Baker E, Kirk K. 2014. Diverse chemotypes disrupt ion homeostasis in the malaria parasite. *Mol Microbiol* 94:327–339. <https://doi.org/10.1111/mmi.12765>
 50. Jiménez-Díaz MB, Ebert D, Salinas Y, Pradhan A, Lehane AM, Myrand-Lapierre M-E, O'Loughlin KG, Shackelford DM, Justino de Almeida M, Carrillo AK, Clark JA, Dennis ASM, Diep J, Deng X, Duffy S, Endsley AN, Fedewa G, Guiguemde WA, Gómez MG, Holbrook G, Horst J, Kim CC, Liu J, Lee MCS, Matheny A, Martínez MS, Miller G, Rodríguez-Alejandre A, Sanz L, Sigal M, Spillman NJ, Stein PD, Wang Z, Zhu F, Waterson D, Knapp S, Shelat A, Avery VM, Fidock DA, Gamo F-J, Charman SA, Mirsalis JC, Ma H, Ferrer S, Kirk K, Angulo-Barturen I, Kyle DE, DeRisi JL, Floyd DM, Guy RK. 2014. +)-SJ733, a clinical candidate for malaria that acts through ATP4 to induce rapid host-mediated clearance of *Plasmodium*. *Proc Natl Acad Sci U S A* 111:E5455–62. <https://doi.org/10.1073/pnas.1414221111>
 51. Sanchez CP, Manson EDT, Moliner Cubel S, Mandel L, Weidt SK, Barrett MP, Lanzer M. 2022. The knock-down of the chloroquine resistance transporter PfCRT is linked to oligopeptide handling in *Plasmodium falciparum*. *Microbiol Spectr* 10:e0110122. <https://doi.org/10.1128/spectrum.01101-22>
 52. Murithi JM, Owen ES, Istvan ES, Lee MCS, Ottilie S, Chibale K, Goldberg DE, Winzeler EA, Llinás M, Fidock DA, Vanaerschoot M. 2020. Combining stage specificity and metabolomic profiling to advance antimalarial drug discovery. *Cell Chem Biol* 27:158–171. <https://doi.org/10.1016/j.chembiol.2019.11.009>
 53. White NJ, Duong TT, Uthaisin C, Nosten F, Phyo AP, Hanboonkunupakarn B, Pukrittayakamee S, Jittamala P, Chuthasmit K, Cheung MS, Feng Y, Li R, Magnusson B, Sultan M, Wieser D, Xun X, Zhao R, Diagona TT, Pertel P, Leong FJ. 2016. Antimalarial activity of KAF156 in *falciparum* and *vivax* malaria. *N Engl J Med* 375:1152–1160. <https://doi.org/10.1056/NEJMoa1602250>
 54. LaMonte G, Lim MY-X, Wree M, Reimer C, Nachon M, Corey V, Gedeck P, Plouffe D, Du A, Figueroa N, Yeung B, Bifani P, Winzeler EA. 2016. Mutations in the *Plasmodium falciparum* cyclic amine resistance locus (PfCARL) confer multidrug resistance. *mBio* 7:e00696-16. <https://doi.org/10.1128/mBio.00696-16>
 55. LaMonte GM, Rocamora F, Marapana DS, Gnädig NF, Ottilie S, Luth MR, Worgall TS, Goldgof GM, Mohunlal R, Santha Kumar R, Thompson JK, Vigil E, Yang J, Hutson D, Johnson T, Huang J, Williams RM, Zou BY, Cheung AL, Kumar P, Egan TJ, Lee MCS, Siegel D, Cowman AF, Fidock DA, Winzeler EA. 2020. Pan-active imidazolidinone antimalarials target the *Plasmodium falciparum* intracellular secretory pathway. *Nat Commun* 11:1780. <https://doi.org/10.1038/s41467-020-15440-4>
 56. Spillman NJ, Allen RJW, McNamara CW, Yeung BKS, Winzeler EA, Diagona TT, Kirk K. 2013. Na⁽⁺⁾ regulation in the malaria parasite *Plasmodium falciparum* involves the cation ATPase PfATP4 and is a target of the spiroindolone antimalarials. *Cell Host Microbe* 13:227–237. <https://doi.org/10.1016/j.chom.2012.12.006>
 57. Wang J, Zhang C-J, Chia WN, Loh CCY, Li Z, Lee YM, He Y, Yuan L-X, Lim TK, Liu M, Liew CX, Lee YQ, Zhang J, Lu N, Lim CT, Hua Z-C, Liu B, Shen H-M, Tan KSW, Lin Q. 2015. Haem-activated promiscuous targeting of artemisinin in *Plasmodium falciparum*. *Nat Commun* 6:10111. <https://doi.org/10.1038/ncomms10111>
 58. Ismail HM, Barton V, Phanchana M, Charoensutthivarakul S, Wong MHL, Hemingway J, Biagini GA, O'Neill PM, Ward SA. 2016. Artemisinin activity-based probes identify multiple molecular targets within the asexual stage of the malaria parasites *Plasmodium falciparum* 3D7. *Proc Natl Acad Sci U S A* 113:2080–2085. <https://doi.org/10.1073/pnas.1600459113>
 59. Xia J, Sinelnikov IV, Han B, Wishart DS. 2015. MetaboAnalyst 3.0—making metabolomics more meaningful. *Nucleic Acids Res* 43:W251–7. <https://doi.org/10.1093/nar/gkv380>
 60. Lambros C, Vanderberg JP. 1979. Synchronization of *Plasmodium falciparum* erythrocytic stages in culture. *J Parasitol* 65:418–420.
 61. Kim CC, Wilson EB, DeRisi JL. 2010. Improved methods for magnetic purification of malaria parasites and haemozoin. *Malar J* 9:17. <https://doi.org/10.1186/1475-2875-9-17>
 62. Srivastava A, Creek DJ, Evans KJ, De Souza D, Schofield L, Müller S, Barrett MP, McConville MJ, Waters AP. 2015. Host reticulocytes provide metabolic reservoirs that can be exploited by malaria parasites. *PLoS Pathog* 11:e1004882. <https://doi.org/10.1371/journal.ppat.1004882>
 63. Creek DJ, Jankevics A, Breitling R, Watson DG, Barrett MP, Burgess KEV. 2011. Toward global metabolomics analysis with hydrophilic interaction liquid chromatography-mass spectrometry: improved metabolite identification by retention time prediction. *Anal Chem* 83:8703–8710. <https://doi.org/10.1021/ac2021823>
 64. van der Hooft JJJ, Padmanabhan S, Burgess KEV, Barrett MP. 2016. Urinary antihypertensive drug metabolite screening using molecular networking coupled to high-resolution mass spectrometry fragmentation. *Metabolomics* 12:125. <https://doi.org/10.1007/s11306-016-1064-z>
 65. Creek DJ, Jankevics A, Burgess KEV, Breitling R, Barrett MP. 2012. IDEOM: an Excel interface for analysis of LC-MS-based metabolomics data. *Bioinformatics* 28:1048–1049. <https://doi.org/10.1093/bioinformatics/bts069>
 66. Smith CA, Want EJ, O'Maille G, Abagyan R, Siuzdak G. 2006. XCMS: processing mass spectrometry data for metabolite profiling using nonlinear peak alignment, matching, and identification. *Anal Chem* 78:779–787. <https://doi.org/10.1021/ac051437y>
 67. Scheltema RA, Jankevics A, Jansen RC, Swertz MA, Breitling R. 2011. PeakML/mzMatch: a file format, java library, R library, and tool-chain for

- mass spectrometry data analysis. *Anal Chem* 83:2786–2793. <https://doi.org/10.1021/ac2000994>
68. Gloaguen Y, Morton F, Daly R, Gurden R, Rogers S, Wandy J, Wilson D, Barrett M, Burgess K. 2017. PiMP my metabolome: an integrated, web-based tool for LC-MS metabolomics data. *Bioinformatics* 33:4007–4009. <https://doi.org/10.1093/bioinformatics/btx499>
69. Sumner LW, Amberg A, Barrett D, Beale MH, Beger R, Daykin CA, Fan T-M, Fiehn O, Goodacre R, Griffin JL, Hankemeier T, Hardy N, Harnly J, Higashi R, Kopka J, Lane AN, Lindon JC, Marriott P, Nicholls AW, Reilly MD, Thaden JJ, Viant MR. 2007. Proposed minimum reporting standards for chemical analysis chemical analysis working group (CAWG) metabolomics standards initiative (MSI). *Metabolomics* 3:211–221. <https://doi.org/10.1007/s11306-007-0082-2>